Outflow Tract Anomalies

11

Leo Lopez, Roque Ventura, and Nadine F. Choueiter

Abstract

Anomalies of the aortic and pulmonary outflow tracts are usually associated with obstruction, regurgitation, and/or aneurysmal dilation of the proximal great arteries, and they represent some of the conditions most frequently encountered by congenital heart disease specialists. In most instances, a full preoperative diagnosis is performed by standard transthoracic echocardiography and other imaging modalities such as cardiac catheterization and magnetic resonance imaging. However, transesophageal echocardiography (TEE) serves an important role in the perioperative management of these patients. Preoperative TEE can provide information regarding the morphology of the outflow tracts and the degree of obstruction and regurgitation; postoperative TEE can evaluate the success of a surgical procedure and exclude residual obstruction, regurgitation, or other potential complications. In addition, TEE is sometimes necessary outside of the operating room setting for older patients with poor transthoracic echocardiographic windows, particularly if the patient has undergone prior surgery. This chapter discusses the use of TEE for the evaluation of both right and left sided outflow tract anomalies.

Keywords

Aortic stenosis, valvar • Aortic stenosis, subvalvar • Aortic stenosis, supravalvar • Aortic regurgitation • Sinus of Valsalva aneurysm • Pulmonary stenosis, valvar • Double-chambered right ventricle • Pulmonary regurgitation

Introduction

Anomalies of the outflow tracts are usually associated with obstruction, regurgitation, and/or aneurysmal dilation of the proximal great arteries. Based on an analysis of almost 40 published articles on the incidence of congenital heart disease spanning many decades, pulmonary stenosis (PS), the most common anomaly of the right ventricular outflow tract (RVOT), ranks as the 4th most common congenital heart disease with a mean incidence of 0.73 per 1,000 live births, and aortic stenosis (AS), the most common anomaly of the left ventricular outflow tract (LVOT), ranks as the 7th most common with a mean incidence of 0.40 per 1,000 live births [1]. Among almost 60,000 patients evaluated at the Cardiovascular Program of Children's Hospital Boston from 1988 to 2002, a pulmonary valve (PV) abnormality was the 4th most common diagnosis with a frequency of 5.7 %, and an aortic valve (AoV) abnormality was the 5th most common with a frequency of 5.5 % [2]. A bicuspid AoV is in fact the most common congenital heart disease with an incidence of 0.4–2 % in the general population [3–5].

L. Lopez, MD (✉) • N.F. Choueiter, MD
Department of Pediatrics,
Albert Einstein College of Medicine,
Children's Hospital at Montefiore,
3415 Bainbridge Ave – Rosenthal 1,
Bronx, NY 10467, USA
e-mail: llmd@llmd.net

R. Ventura, RCS
Department of Pediatrics,
Miami Children's Hospital, 3100 Southwest 62nd Avenue,
Miami, FL 33155, USA

The online version of this chapter (doi:10.1007/978-1-84800-064-3_11) contains supplementary material, which is available to authorized users.

P.C. Wong, W.C. Miller-Hance (eds.), *Transesophageal Echocardiography for Congenital Heart Disease*,
DOI 10.1007/978-1-84800-064-3_11, © Springer-Verlag London 2014

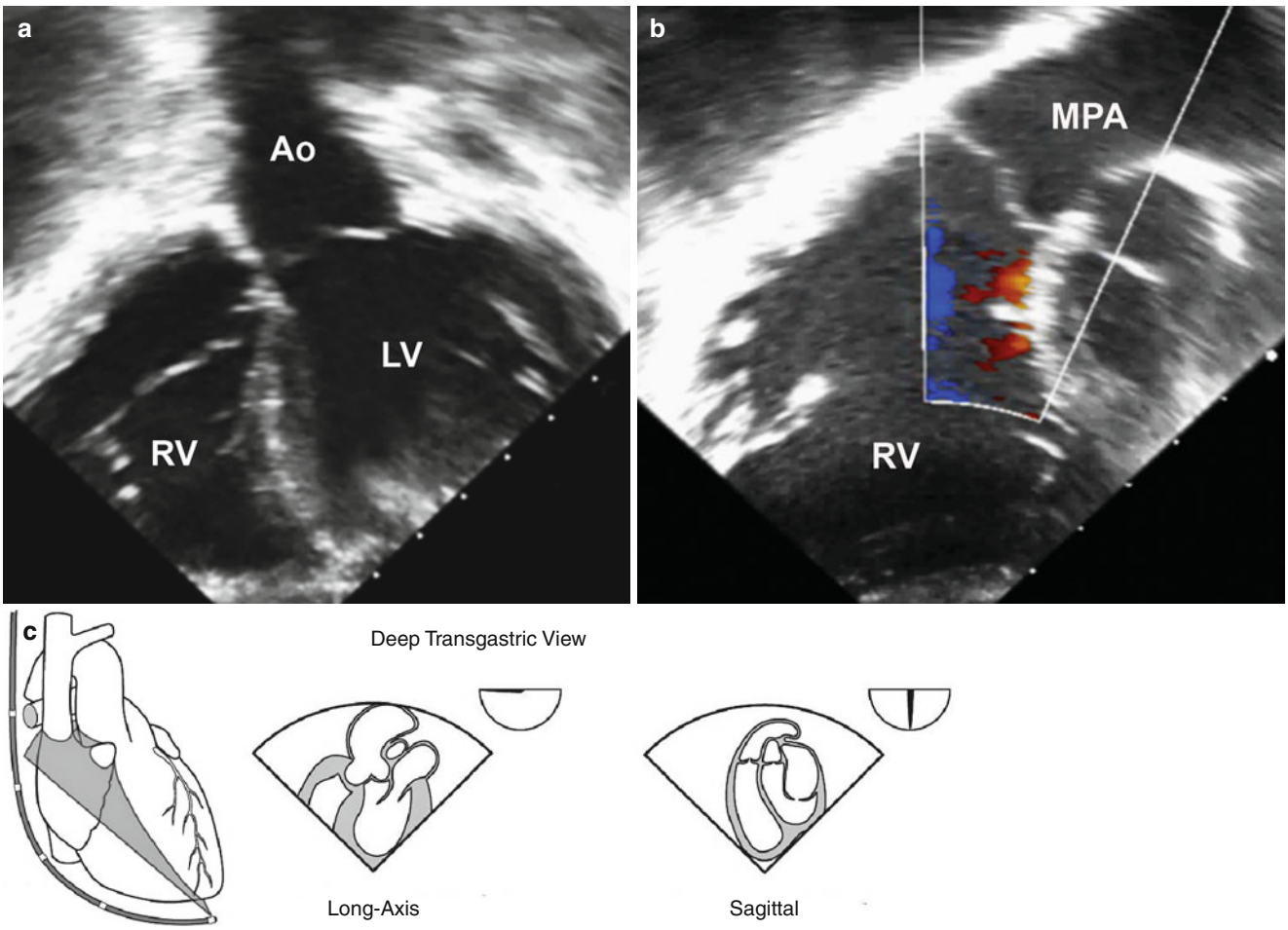

Fig. 11.1 (**a**) Deep transgastric long axis view at 0° showing the LV outflow tract; (**b**) Deep transgastric sagittal view at 90° showing the RV outflow tract; (**c**) Illustration depicting how the LV and RV outflow tracts are evaluated in deep transgastric views (*Ao* aorta, *LV* left ventricle, *MPA* main pulmonary artery, *RV* right ventricle)

Because isolated obstruction at the valvar level in both outflow tracts is generally treated in the catheterization laboratory rather than in the operating room, intraoperative transesophageal echocardiography (TEE) is not frequently performed for valvar stenosis. However, if the obstruction occurs at the subvalvar or supravalvar level or if the primary lesion is regurgitation and/or aneurysmal dilation of the proximal great artery, surgical intervention is often necessary, thereby requiring intraoperative TEE before and after the surgery.

Utility of Transesophageal Echocardiography

Patients with significant outflow tract anomalies other than valvar AS or PS do not usually require surgery during the first year of life, and they often do not undergo any intervention until they are toddlers, adolescents, or adults. Outflow tract obstruction and semilunar valve regurgitation are usually associated with a morphologic abnormality at or near the semilunar valves. During the preoperative evaluation in the operating room, TEE can usually provide information regarding the morphology of the outflow tracts from the mid and upper esophageal views, and the degree of obstruction and regurgitation, if present, from the deep transgastric (Fig. 11.1, Video 11.1a and 11.1b) and mid esophageal views (see Chap. 4) [6]. Postoperative TEE can evaluate the success of a surgical procedure and exclude residual obstruction, regurgitation, or other potential complications. However it is important to note that intraoperative TEE data will always reflect the patient's hemodynamics, which can be affected by general anesthesia, inotropic support, volume status, and ventricular function. For example, the degree of residual obstruction or regurgitation across a semilunar valve can be underestimated in the setting of general anesthesia, hypovolemia, tachycardia, or poor ventricular function. In contrast, the degree of dynamic obstruction, as seen in tetralogy of Fallot or hypertrophic cardiomyopathy secondary to muscular hypertrophy in the subarterial

region, can be overestimated in the presence of hypovolemia or hyperdynamic ventricular function, especially with inotropic support.

Occasionally, TEE is necessary outside of the operating room for older patients with poor transthoracic echocardiographic windows, particularly if the patient has undergone prior surgery.

Normal Anatomy

The term conotruncus (from the Greek words conus for cone and truncus for trunk or body) represents the outflow tracts of both ventricles. It is composed of the subarterial regions, the semilunar valves, the great arterial roots, and the proximal trunks. The conus (also known as the infundibulum from the Latin word for funnel) defines the subarterial muscular chamber, which prevents fibrous continuity between the semilunar valve and the corresponding atrioventricular valve. In the normal heart, the subpulmonary conus prevents fibrous continuity between the tricuspid valve and the PV. The supraventricular crest is the prominent muscular shelf along the posterior aspect of the subpulmonary conus, and it is composed of the conal septum (or infundibular septum) separating the RVOT from the LVOT, the right ventriculo-infundibular fold separating the tricuspid valve leaflets from the PV leaflets, and the subpulmonary muscular sleeve supporting the PV leaflets. The subpulmonary conus is separated from the trabecular segment of the RV chamber at the infundibular os, an area defined by the moderator band, the septal band (also known as the septomarginal trabeculation), and the parietal band of the RV. The subaortic conus regresses *in utero*, resulting in varying degrees of fibrous continuity between the mitral valve and AoV. This fibrous area, known as the mitral-aortic intervalvular fibrosa, is measured as the shortest distance from the anterior mitral leaflet to the base of the non-coronary or left coronary AoV leaflet and can be elongated in cases of subvalvar AS and tetralogy of Fallot.

The normal semilunar valve is a three-dimensional structure wherein three leaflets (or cusps) are attached to the arterial root and supporting ventricular muscle in a semilunar or crown-like fashion. The leaflets are separated by three commissures that extend during diastole from the center of the valve at the level of the ventriculo-arterial junction to the periphery at the level of the sino-tubular junction (Fig. 11.2, Video 11.2). It is important to recognize that the semilunar valve "annulus" is in fact a diagnostician construct without a true anatomic correlate since the semilunar valve leaflet attachments extend from the anatomic ventriculo-arterial junction up to the sino-tubular junction; the so-called "annulus" as defined in echocardiography represents only the most proximal attachment of the semilunar valve and not its attachment in entirety [7] (Fig. 11.3, Video 11.3).

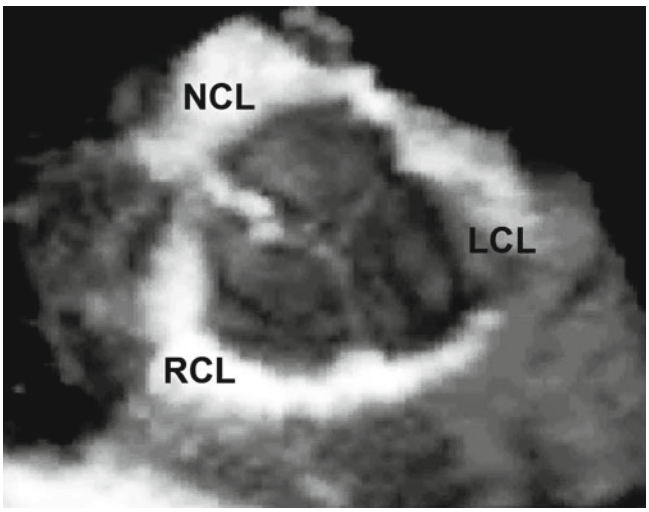

Fig. 11.2 Three-dimension mid esophageal aortic valve short axis view depicting the three-dimensional nature of a normal tri-leaflet aortic valve (*LCL* left coronary leaflet, *NCL* non-coronary leaflet, *RCL* right coronary leaflet)

Left Ventricular Outflow Tract Anomalies

Valvar Aortic Stenosis

Congenital valvar AS results from a bicuspid or unicuspid AoV, a dysplastic tricuspid AoV, or a hypoplastic aortic "annulus". Acquired valvar AS usually results from calcification secondary to degenerative or post-inflammatory causes [8], though a bicuspid AoV is also a risk factor for calcification [5]. A bicuspid AoV is the most common cause of valvar AS, although the presence of a bicuspid AoV does not necessarily mean a patient has (or will develop) valvar AS. As noted previously, a bicuspid AoV is the most common congenital heart defect, with an incidence of 0.4–2 % in the general population [3–5]. There are several distinct anatomic variations. It is rare to encounter a bicuspid AoV with only two well-developed leaflets (Fig. 11.4, Video 11.4); instead, it usually involves fusion of two of the three leaflets or underdevelopment of one of the commissures (known as a raphé) [9]. It is because of the absence of one of the three commissures that the lesion is often referred to as a bicommissural AoV. Among these, fusion occurs most commonly at the intercoronary commissure between the right and left coronary leaflets with a frequency of 70 % (Fig. 11.5, Video 11.5), followed by the commissure between the right and non-coronary leaflets with a frequency of 28 % (Fig. 11.6, Video 11.6); fusion at the commissure between the left and non-coronary leaflets is very rare [10]. In adults, the rate of AS progression appears to be higher in those valves with fusion of the intercoronary commissure [11], though studies in children have revealed more rapid progression of AS and regurgitation as well as shorter time from diagnosis to

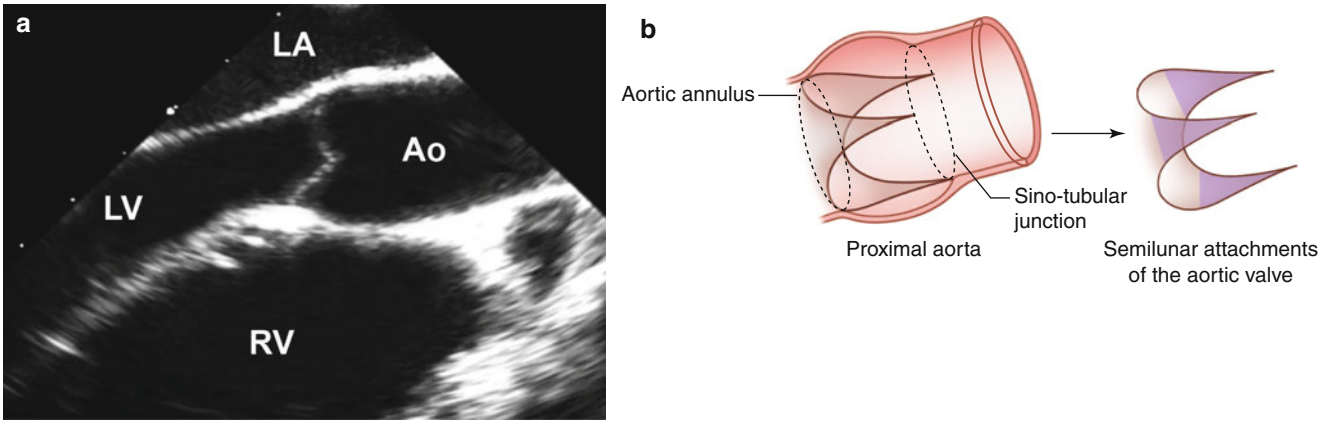

Fig. 11.3 (**a**) Mid esophageal aortic valve long axis view at 120° showing the LV outflow tract; (**b**) Illustration of the aortic valve and its semilunar attachments within the aortic root from the ventriculo-arterial junction to the sino-tubular junction (*Ao* aorta, *LA* left atrium, *LV* left ventricle, *RV* right ventricle)

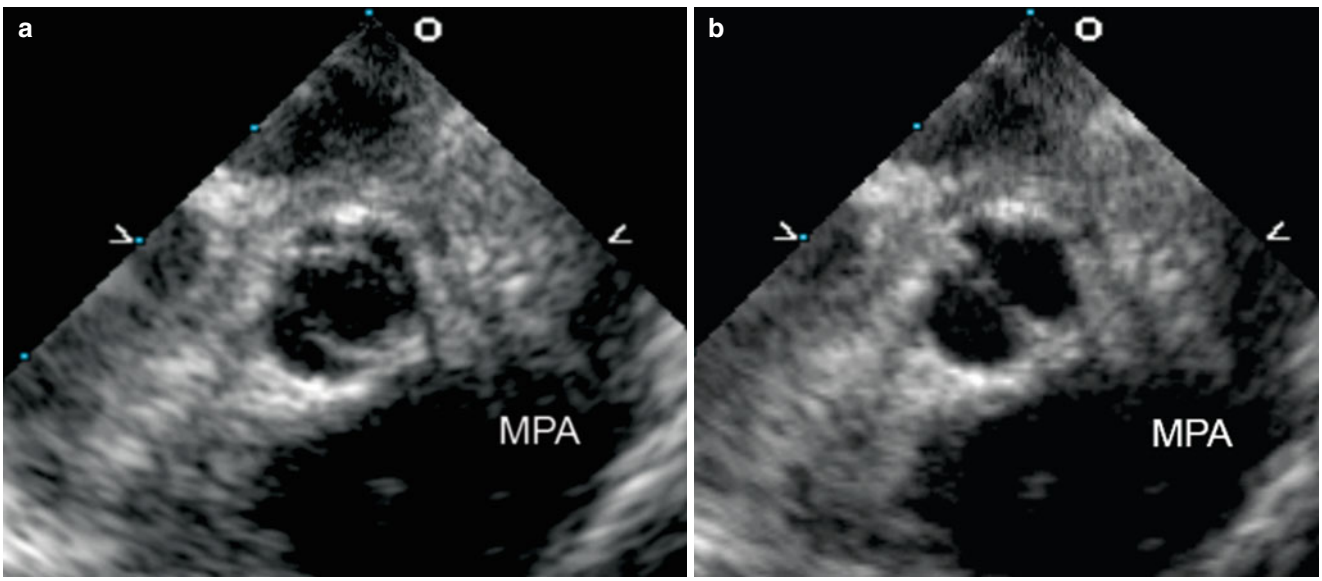

Fig. 11.4 Mid esophageal aortic valve short axis view at 30° shows a true bicuspid aortic valve with only two leaflets (the right and left coronary leaflets) and absent non-coronary leaflet, in the open (**a**) and closed (**b**) positions. This gives a "fishmouth" appearance to the valve orifice (*MPA* main pulmonary artery)

intervention in valves with fusion of the commissure between the right and non-coronary leaflets [12]. Associations with a bicuspid AoV include aortic coarctation [3] or interrupted aortic arch, subvalvar AS, a ventricular septal defect (VSD), a coronary anomaly, Turner syndrome [13], and aortic dilation or aneurysm formation [14–16]. Valvar AS can be an evolving pathology and the degree of progression may be associated with age at presentation and/or severity at the time of presentation [17]. Although it occurs rarely, sudden death in this patient population appears to be related to significant stenosis and regurgitation [18]. In addition, the chronic pressure load experienced by the LV leads to hypertrophy with the potential for permanent muscular damage and fibrosis. Therefore, management of these patients must focus on prevention of these sequelae.

Over the past several decades, transcatheter balloon valvotomy in the catheterization laboratory has become a more popular management approach for patients with valvar AS, superseding surgical valvotomy as the primary mode of treatment. TEE is not often needed during this procedure, though occasionally it is helpful in determining the appropriate intervention and/or assessing its efficacy. Echocardiography for valvar AS should always include assessment of leaflet and commissural morphology, degree of obstruction, degree of LV

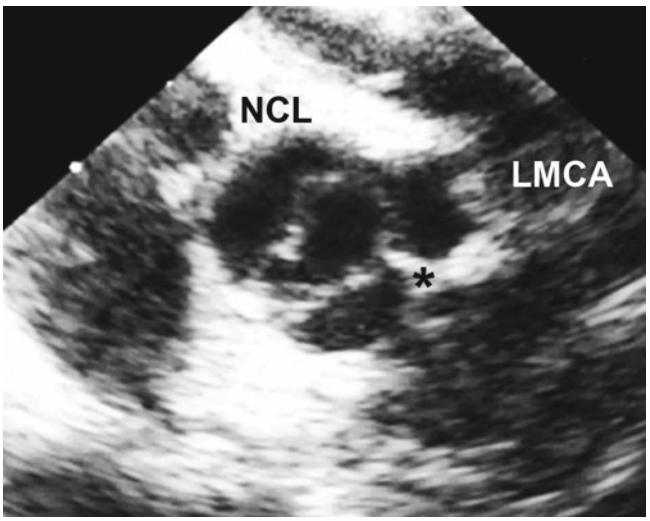

Fig. 11.5 Mid esophageal aortic valve short axis view at 30° showing a bicuspid aortic valve with fusion or underdevelopment of the intercoronary commissure (*black asterisk*) (*NCL* non-coronary leaflet, *LMCA* left main coronary artery)

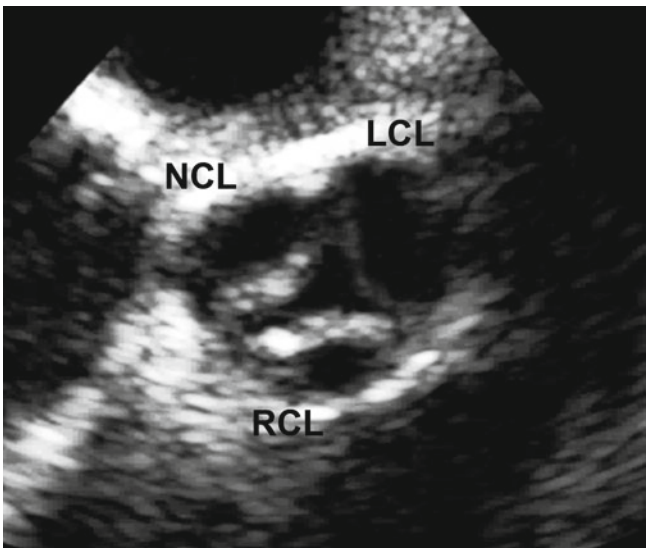

Fig. 11.7 Mid esophageal aortic valve short axis view at 30° showing a dysplastic aortic valve with thickened right and non-coronary leaflets (*LCL* left coronary leaflet, *NCL* non-coronary leaflet, *RCL* right coronary leaflet)

Fig. 11.6 Mid esophageal aortic valve short axis view at 30° showing a bicuspid aortic valve with fusion or underdevelopment of the commissure between the right and non-coronary leaflets (*black asterisk*) (*LCL* left coronary leaflet)

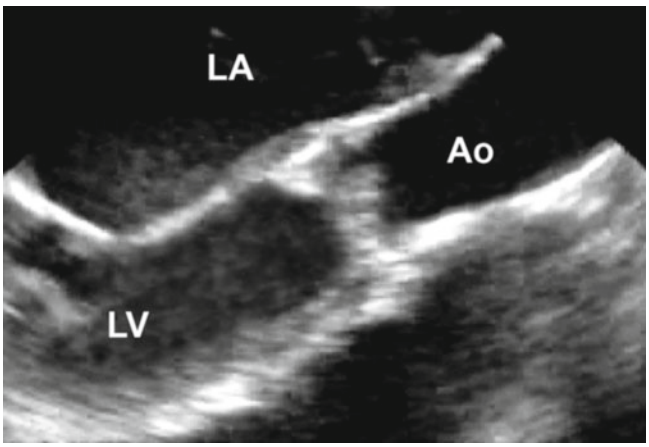

Fig. 11.8 Mid esophageal aortic valve long axis view at 120° showing a dysplastic aortic valve associated with valvar aortic stenosis (*Ao* aorta, *LA* left atrium, *LV* left ventricle)

hypertrophy, ascending aortic size, and left atrial dilation. Aortic measurements (aortic valve, aortic root, and ascending aorta) are often helpful. Leaflet and commissural morphology are best evaluated in the mid esophageal views, usually at 30–45° for the mid esophageal aortic valve short axis (ME AV SAX) images (Figs. 11.4, 11.5, 11.6, and 11.7, Videos 11.4, 11.5, 11.6, and 11.7) and at ~120° for the mid esophageal aortic valve long axis (ME AV LAX) images (Fig. 11.8, Video 11.8). It is, however, important to recognize that pure short and long axis images can be difficult to obtain—even with multiplane TEE—because of the fixed spatial relationship between the esophagus and the aortic outflow tract. When a pure short axis image is available (that is, when the AoV annular plane is completely perpendicular to the axis of the beam), the relative sizes of the leaflets should be evaluated, and failure of commissural opening in the setting of a bicuspid or unicuspid valve can be displayed. Long axis imaging of the AoV can reveal thickened and doming leaflets. More recently, three-dimensional echocardiography has emerged as an important tool for the assessment of aortic valve anatomy and pathology (Chaps. 19 and 20).

The degree of obstruction is generally assessed by estimation of the pressure gradient across the stenotic valve, using continuous wave Doppler interrogation along the aortic outflow tract. This is best performed in the deep transgastric long axis (DTG LAX) view with multiplane angle between 0° and 30° (Fig. 11.1a, Video 11.1a), or sometimes from the deep transgastric sagittal (DTG Sagittal) view with multiplane angle between 80° and 110° (Fig. 11.1b, Video 11.1b).

Because of the distance from the probe to the outflow tract, imaging from this view often requires using the lowest possible frequency for improved penetration as well as minimizing the image and color sector size. Every effort should be made to align the Doppler beam with the LVOT. As an alternative, the transgastric long axis view (TG LAX) can be used for interrogation of the LVOT because it generally provides favorable angles for continuous wave Doppler interrogation (Chap. 4) with a shorter distance from the probe to the aortic valve. Both peak and mean pressure gradients should be measured [19–21]. It is important to recognize that echocardiographically derived Doppler gradients often do not correspond to the peak-to-peak gradient measured in the catheterization laboratory, a common discrepancy which results from several factors, including a phenomenon called pressure recovery [22]. In addition, severe LV dysfunction in the setting of valvar AS is associated with low cardiac output and diminished transvalvar flow, and Doppler interrogation may reveal a low gradient despite severe obstruction at the valvar level. Similarly, the degree of LVOT obstruction can be artificially decreased in the setting of general anesthesia, deep sedation, or hypovolemia. In addition to pressure gradient, some use calculated aortic valve area to evaluate the degree of obstruction as derived by the continuity equation, which states that the stroke volume in the subaortic region is the same as the stroke volume at the valvar level (see Chap. 1). Since stroke volume is equal to the velocity-time integral multiplied by cross-sectional area at a particular location, the effective aortic valve area can be calculated if the LVOT cross-sectional area and the velocity-time integrals at the LVOT and at the aortic valve are known [23]. However, the LVOT is frequently not circular in shape, precluding accurate assessment of LVOT cross-sectional areas using LVOT diameters, and some have suggested that three-dimensional TEE may be preferable to two-dimensional imaging for more accurate assessments of aortic valve area [24].

It is important to note that AS represents a disease continuum, and severity cannot be defined by a single value [21]. With these considerations in mind, the following echocardiographic criteria for classification of AoV stenosis severity were recently given by a 2008 American College of Cardiology/American Heart Association (ACC/AHA) task force on valvular heart disease [21].

- Mild: peak velocity <3 m/s, mean gradient <25 mmHg, valve area >1.5 cm^2
- Moderate: peak velocity 3.0–4.0 m/s, mean gradient 25–40 mmHg, valve area 1.0–1.5 cm^2
- Severe: peak velocity >4 m/s, mean gradient >40 mmHg, valve area <1.0 cm^2

Similar guidelines have not been written specifically for the pediatric population. At present, the above criteria are generally applied to this group of patients as well [25–27].

LV hypertrophy is best evaluated in the transgastric basal short axis (TG Basal SAX) and transgastric mid short axis (TG Mid SAX) views at 0°, though a quantitative assessment of the degree of hypertrophy may not be reliable with TEE, again because pure short axis images of the LV in transgastric views at 0° may not always be available. The size of the aortic root and ascending aorta are best measured in mid esophageal aortic valve long axis (ME AV LAX) and mid esophageal ascending aortic long axis (ME Asc Ao LAX) views at 90–120°; important measurements that should be obtained in early to mid systole include the diameters of the aortic valve annulus, aortic root diameter, sino-tubular junction, and ascending aorta [28]. These measurements are analogous to those obtained by transthoracic echocardiography, and they can be compared to published normal values [29, 30]. Left atrial dilation can be easily visualized in mid esophageal fourchamber (ME 4 Ch) and twochamber (ME 2 Ch) views at 0° and 90° respectively.

Recently, a new procedure for the nonsurgical treatment of severe valvar AS has garnered widespread interest. Known as transcatheter AoV replacement/implantation, or TAVR/TAVI, this procedure is performed in the cardiac catheterization laboratory and involves the implantation of a bovine or porcine pericardial valve mounted upon a metal support frame [31]. Delivered transarterially (access by percutaneous femoral or subclavian artery, or through the left ventricular apex), the balloon-mounted valve is advanced to the AoV position, and the balloon expanded within the diseased AoV, displacing the diseased native valve leaflets. During the procedure, TEE is utilized and serves a number of important functions: (a) pre-procedure evaluation of anatomy and function; (b) monitoring of valve implantation; (c) post-implantation evaluation of valve function and valve regurgitation (Fig. 11.9, Video 11.9). The post-implantation TEE is particularly useful in that it enables accurate differentiation between transvalvar and paravalvar aortic regurgitation, something not easily visualized by angiography or fluoroscopy [32]. At present, two major valves are available—the Edwards SAPIEN XT heart valve (Edwards Lifesciences Inc., Irvine, California) and the CoreValve ReValving system (Medtronic Inc., Minneapolis, Minnesota)—but a number of other valves are undergoing early clinical evaluation [33]. Currently, the procedure is performed only in adults; candidates are generally patients with severe valvar AS felt to be too high risk for surgical intervention [34, 35] (see also Chap. 16).

Subvalvar Aortic Stenosis

Subvalvar AS is rarely diagnosed *in utero* or in the newborn period, prompting many people to classify this lesion as an acquired heart disease rather than a congenital one [36, 37]. It is a progressive disease, particularly in children, and some have suggested that its development may involve the following mechanisms: abnormal LVOT morphology leads to increased septal shear stress, which because of some genetic predisposition leads in turn to cellular proliferation [38, 39]. Some of the abnormalities in LVOT morphology that are

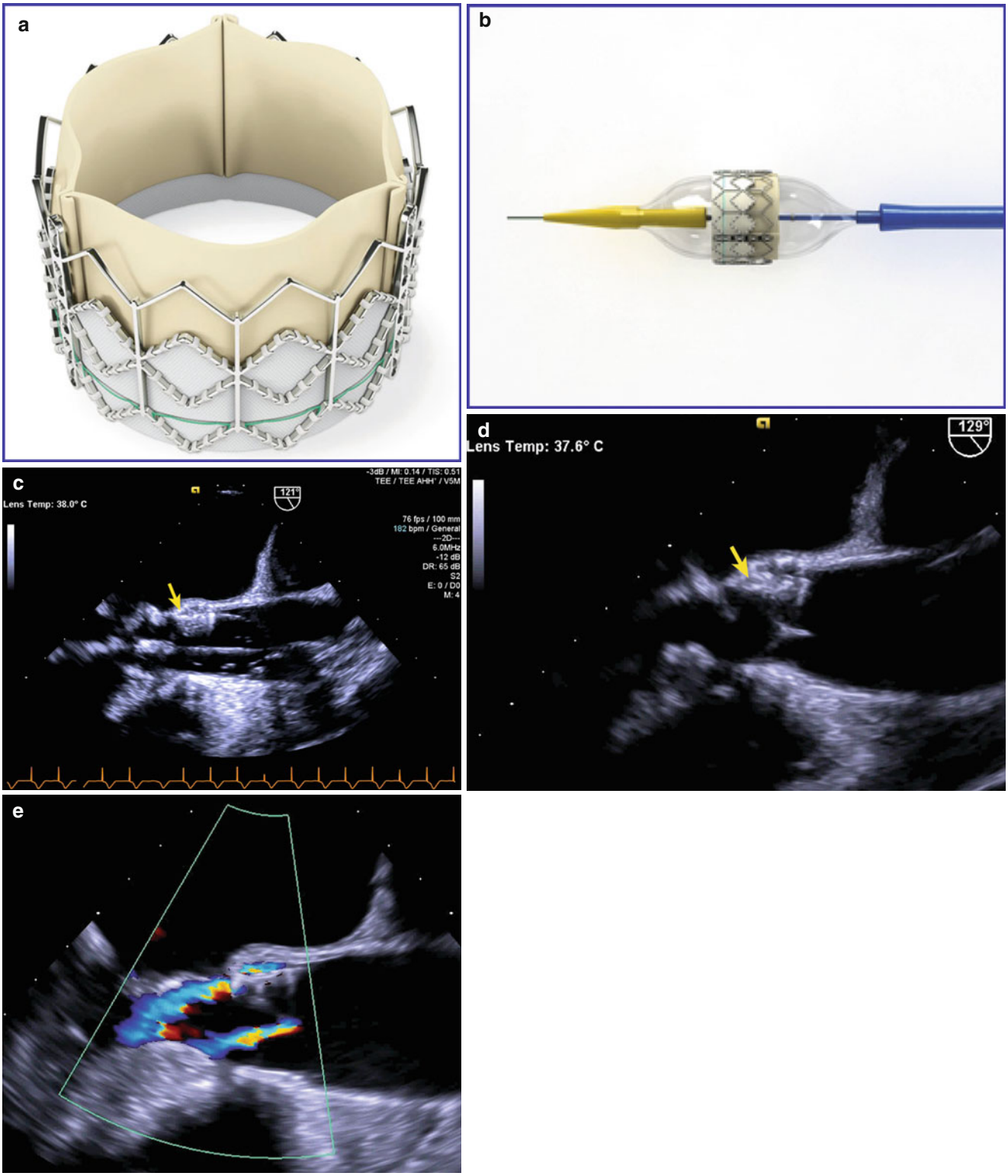

Fig. 11.9 Transcatheter aortic valve replacement/implantation (TAVR/TAVI). (**a**) Shows the Edwards SAPIEN valve (Edwards Lifesciences Inc., Irvine, California), a bovine pericardial valve mounted on a stainless steel frame. (**b**) Shows the same valve mounted on a balloon catheter that is used for valve delivery. (**c**–**e**) Are transesophageal echocardiographic images obtained from the mid esophageal aortic valve long axis view at 120–130°. (**c**) Shows the balloon being inflated (device indicated with *arrow*), and (**d**) Shows the valve (*arrow*) after implantation. In (**e**), following valve implantation color flow Doppler shows two small jets of regurgitation: one a central transvalvar jet, the other a peripheral paravalvar jet (Echocardiographic images provided courtesy of Siemens Medical Systems USA, Inc. © 2012–13 Siemens Medical Solutions USA, Inc. All rights reserved)

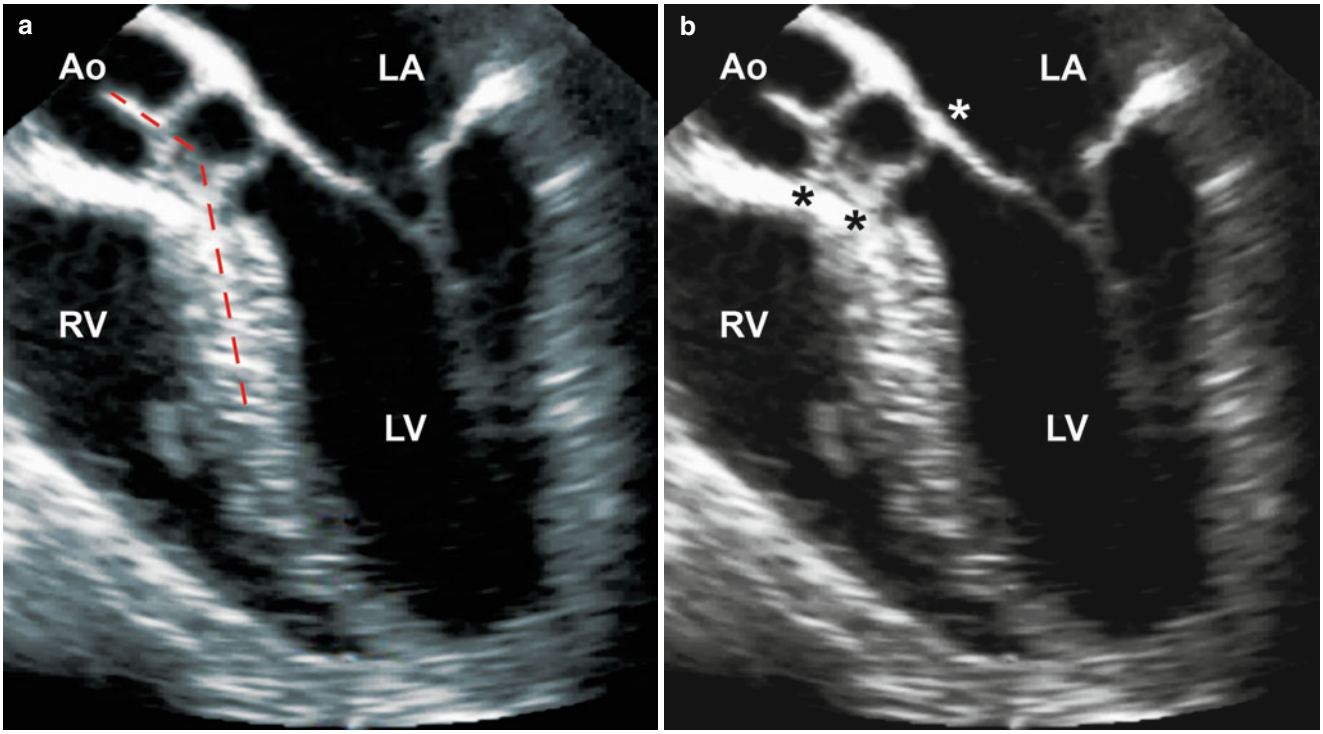

Fig. 11.10 Mid esophageal four chamber view with probe anteflexion to visualize the left ventricular outflow tract, showing a subaortic fibromuscular ridge associated with subvalvar aortic stenosis. The two figures depict (**a**) a steep aorto-septal angle (*dashed red lines*), and (**b**) the distance between the ridge and the aortic annulus (*black asterisk*) and extension of the fibromuscular ridge to the anterior mitral leaflet (*white asterisk*) (*Ao* aorta, *LA* left atrium, *LV* left ventricle, *RV* right ventricle)

associated with subvalvar AS include a steep aorto-septal angle (Fig. 11.10a, Video 11.10), an elongated mitral-aortic intervalvular fibrosa, exaggerated aortic override [40, 41], prominent LVOT muscle bundles, and abnormal mitral valve attachments to the ventricular septum. In addition, the distance from the level of the obstruction to the AoV appears to be one of the major predictors of significantly progressive obstruction [42] (Fig. 11.10b, Video 11.10). Subvalvar AS can occur without or with a VSD. Examples of subvalvar AS in the absence of a VSD include: (a) a discrete fibrous or fibromuscular subaortic ridge protruding from the ventricular septum and sometimes extending to the anterior mitral leaflet (Fig. 11.10b, Video 11.10); (b) an extensive muscular shelf creating a tunnel-like LVOT; (c) hypertrophic cardiomyopathy with dynamic obstruction secondary to diffuse septal hypertrophy and systolic anterior motion of the mitral valve and/or its tensor apparatus (Fig. 11.11, Video 11.11). Subvalvar AS without a VSD can also develop postoperatively after mitral valve replacement with a mechanical prosthesis [43–45]. The most common type of subvalvar AS in the setting of a VSD occurs with posterior deviation of the conal septum, a lesion that is often associated with aortic coarctation or interrupted aortic arch [46, 47]. (see Chaps. 9 and 13) Other examples of subvalvar AS include endocardial folds or fibromuscular ridges at the crest of the muscular septum (Fig. 11.12, Video 11.12), often without significant obstruction [48], and abnormal mitral valve attachments to the ventricular septum, often in the setting of an atrioventricular canal (atrioventricular septal) defect (see Chap. 8) Aside from a VSD, subvalvar AS can also be associated with a bicuspid AoV, a double-chambered RV (DCRV) [49], and aortic regurgitation (AR). In fact, the risk for rapidly progressive AR is frequently the reason that children with subvalvar AS require early surgical intervention [50], although AR in adults with subvalvar AS is rarely progressive [51, 52].

TEE is especially useful in delineating the mechanism of obstruction in patients with subvalvar AS. A fibromuscular ridge with or without extension to the anterior mitral leaflet, posterior deviation of the conal septum, a tunnel-like LVOT, and abnormal mitral valve attachments to the ventricular septum can usually be characterized in the ME 4 Ch and ME AV LAX (at ~120°) views or in the DTG LAX view at 0–30° and DTG Sagittal view at 80–110°. In addition, the distance from a fibromuscular ridge to the AoV leaflets can be measured in these views (Fig. 11.10b). The degree of AR can usually be assessed in multiple mid esophageal and deep transgastric views (as discussed later in this chapter). The AoV leaflet and commissural morphology should always be evaluated in the ME AV SAX view at ~30° (Figs. 11.4, 11.5, 11.6, and 11.7), especially in the setting of significant AR. The utility and limitations of the DTG LAX view at 0–30° in quantifying the

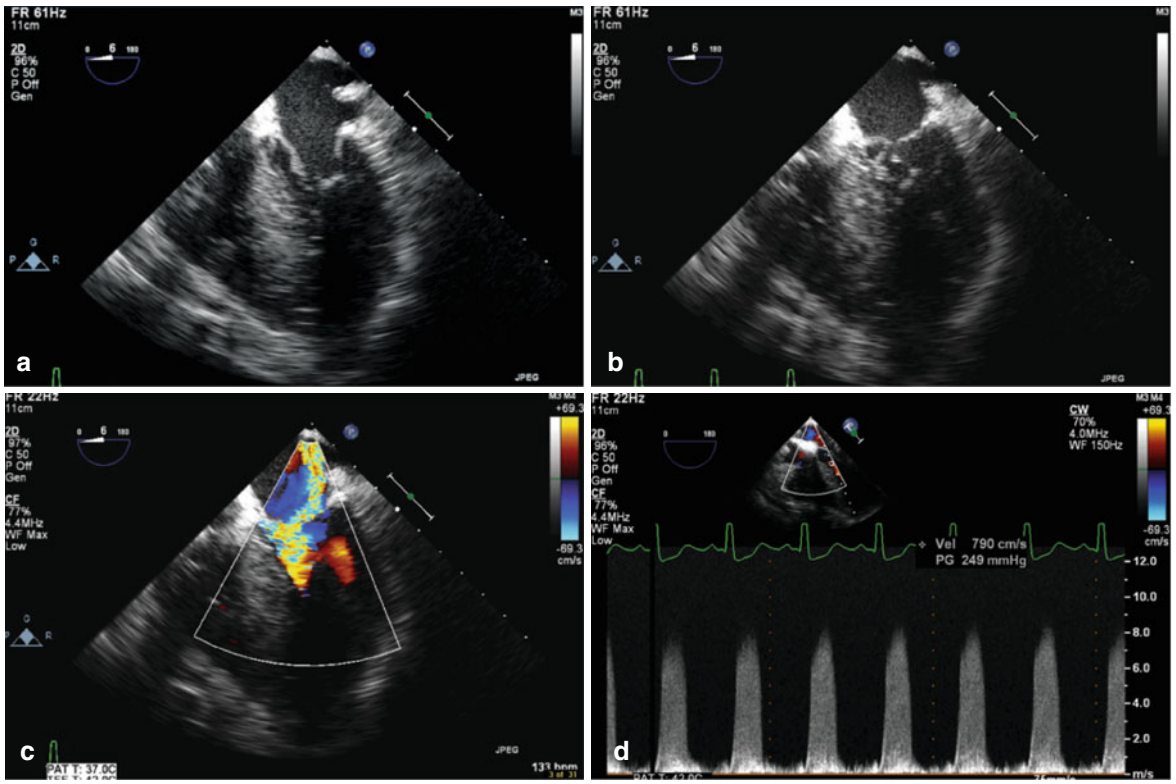

Fig. 11.11 Mid esophageal four chamber view showing subaortic stenosis causing systolic anterior motion (SAM) of the mitral valve, in a patient with significant ventricular septal hypertrophy. This is characterized by systolic displacement of the anterior mitral leaflet into the left ventricular outflow tract. In diastole (**a**) the mitral valve opens normally. However during systole there is a "drag" effect produced by the underfilled, hyperdynamic left ventricle that pulls the anterior leaflet into the left ventricular outflow tract (**b**). This prevents the mitral valve from effective coaptation and produces significant mitral regurgitation (**c**). The SAM also results in dynamic left ventricular outflow tract obstruction, producing a gradient that can be very high; in this patient there is a late-peaking, dagger-shaped spectral Doppler tracing, with a peak velocity measured at nearly 8 m/s, or 256 mmHg (**d**)

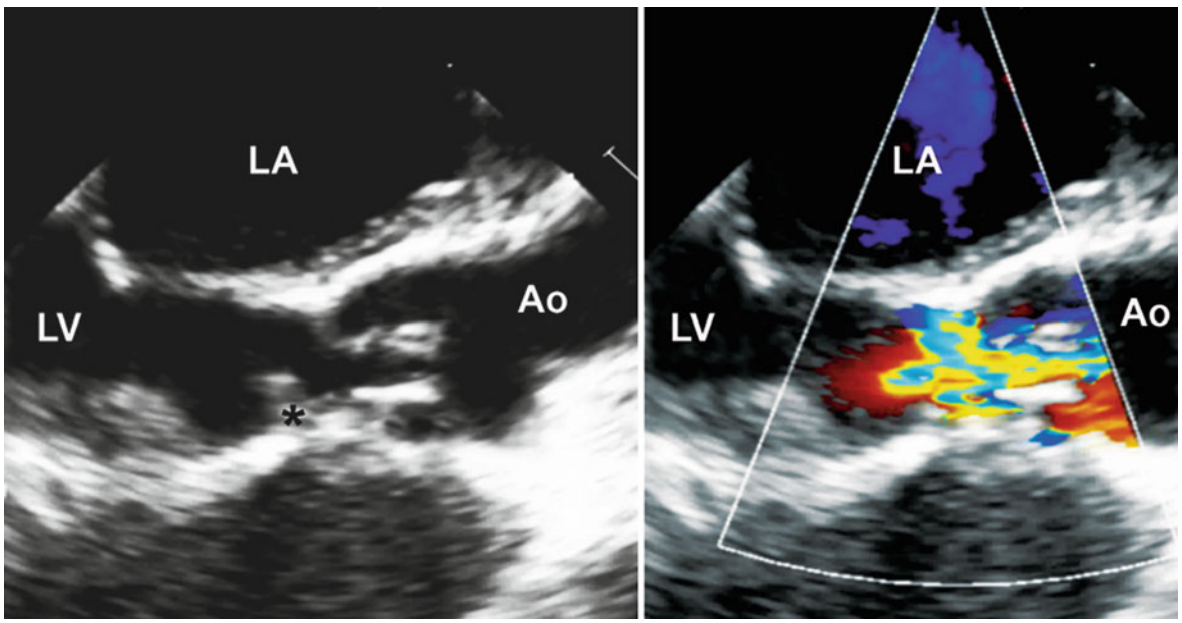

Fig. 11.12 Mid esophageal aortic valve long axis view at 120° showing a subaortic fibromuscular ridge (*black asterisk*) and a dysplastic aortic valve resulting in combined subvalvar and valvar aortic stenosis in addition to a small membranous ventricular septal defect (not well-seen on the image, but readily visible on Video 11–12). The fibromuscular ridge is located at the crest of the muscular septum. *Ao* aorta, *LA* left atrium, *LV* left ventricle

degree of obstruction have been discussed previously. Occasionally a ME Asc Ao LAX view at ~120°, or higher view such as the upper esophageal aortic arch long axis (UE Ao Arch LAX) at 0° or upper esophageal aortic arch short axis (UE Ao Arch SAX) at ~120° can provide an adequate Doppler angle to measure the gradient arising from the subaortic region. In some instances of subvalvar AS, a favorable angle for spectral Doppler interrogation can even be obtained from a modified ME 4 Ch view (Fig. 11.11, Video 11.11), though care must be taken not to contaminate the continuous wave Doppler tracing with a mitral regurgitation jet present along the same scan line. After mitral valve replacement with a mechanical prosthesis, the mid esophageal window can be ineffective because the mechanical prosthesis is located between the TEE probe and the LVOT, and acoustic interference by the prosthesis can partially or completely inhibit visualization of the outflow tract. In these instances, the TG LAX and deep transgastric views (DTG LAX, DTG Sagittal) can be helpful since the probe is positioned beyond the prosthesis, allowing for unobstructed imaging and Doppler interrogation. Associations such as a VSD or a DCRV should be excluded in the preoperative TEE, and these are usually visualized in the mid esophageal views: the ME 4 Ch view at 0° and the mid esophageal right ventricular inflow-outflow (ME RV In-Out) at 60–90°. Postoperatively, residual LVOT obstruction should be excluded qualitatively in the ME AV LAX and mid esophageal long axis (ME LAX) views (multiplane angle for both at ~120°), and quantitatively (by spectral Doppler evaluation) in the DTG LAX, DTG Sagittal, and TG LAX views. The AoV leaflets should be re-evaluated in the ME AV SAX view at 30–45°, and the presence of post-interventional AR should be assessed in multiple mid esophageal and deep transgastric views. Finally, inadvertent VSD creation and/or mitral valve injury are known complications following surgical intervention of subvalvar aortic stenosis [53, 54]. These areas should be evaluated carefully by postoperative TEE using a variety of mid esophageal and deep transgastric views, as described above and in Chap. 4.

Supravalvar Aortic Stenosis

Supravalvar AS is the least common type of LVOT obstruction, representing only 7 % of all patients undergoing surgical repair for LVOT obstruction at Children's Hospital Boston from 1956 to 1976 [55]. Although it occasionally presents as a familial autosomal dominant lesion or as a sporadic idiopathic disorder, it is usually associated with Williams syndrome, a constellation of clinical features which include developmental delay, calcium metabolism problems, failure to thrive, and abnormal facial features [56]. Supravalvar AS results from a mutation or deletion of the elastin gene on chromosome 7 [57, 58]. The obstruction occurs at the sino-tubular junction, and

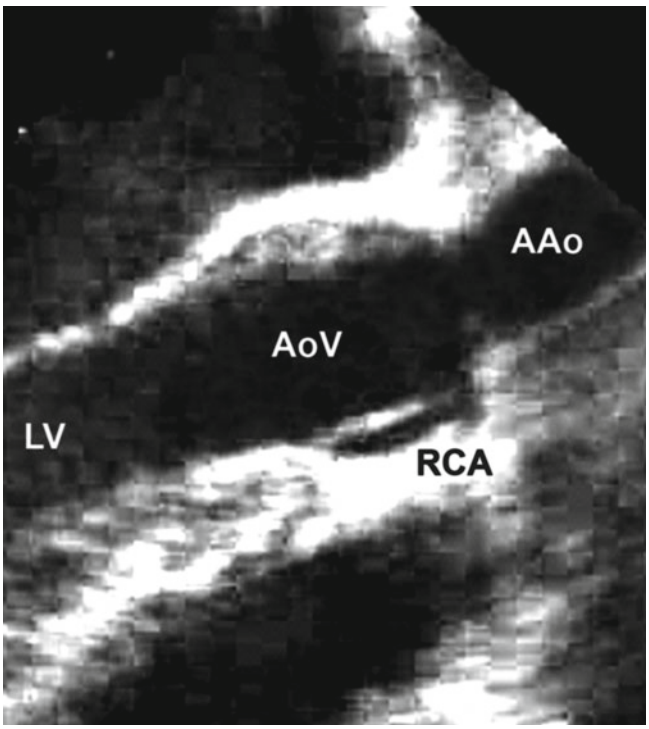

Fig. 11.13 Mid esophageal aortic valve long axis view at 120° showing discrete narrowing at the sino-tubular junction resulting in supravalvar aortic stenosis and entrapment of the right coronary ostium (*AAo* ascending aorta, *AoV* aortic valve, *LV* left ventricle, *RCA* right coronary artery)

three anatomic subtypes have been described: the hourglass type (most common) involving dilation of the aortic root proximal to the narrowing and the ascending aorta distal to the narrowing (Fig. 11.13, Video 11.13), the membranous or diaphragmatic type, and the rare tubular type with diffuse hypoplasia of the ascending aorta [59, 60]. Patients with Williams syndrome can also have branch pulmonary artery stenosis, aortic coarctation, and renal artery stenosis in addition to supravalvar AS. Other associations include subvalvar AS, an abnormal AoV, and coronary abnormalities such as coronary artery dilation, coronary thickening, ostial stenosis, and ostial entrapment by a tethered AoV (Fig. 11.13). Obstruction can occur at more than one level, and the degree of obstruction usually progresses over time. Surgical intervention is generally undertaken when significant obstruction is present in order to prevent irreversible left ventricular myocardial damage. In many cases, TEE is superior to transthoracic echocardiography in the evaluation of the entire extent of the ascending aorta. The aortic root and proximal ascending aorta are best assessed by TEE in a ME AV LAX view at ~120° wherein the long axis of the proximal aorta can be displayed (Fig. 11.13, Video 11.13). During probe withdrawal in this view, the ascending aorta can be further evaluated with the ME Asc Ao LAX view. The degree of obstruction can be quantified with

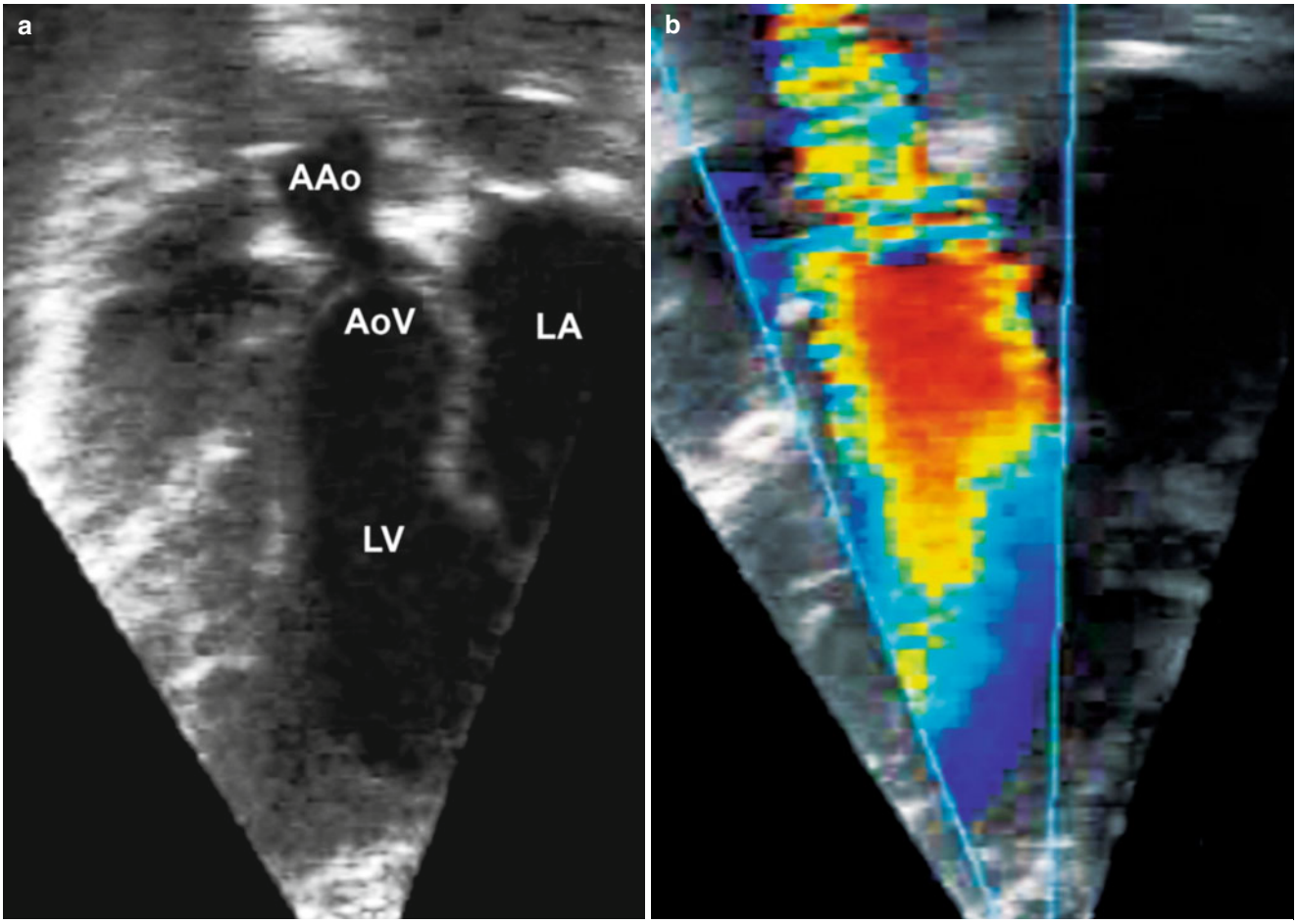

Fig. 11.14 Deep transgastric long axis view at 30° showing discrete narrowing of the sino-tubular junction resulting in supravalvar aortic stenosis (**a**) two-dimensional imaging and (**b**) color flow mapping (*AAo* ascending aorta, *AoV* aortic valve, *LA* left atrium, *LV* left ventricle)

DTG LAX (Fig. 11.14, Video 11.14), DTG Sagittal, and TG LAX views. In some cases, withdrawing the probe to an UE Ao Arch LAX or UE Ao Arch SAX view will provide an adequate Doppler angle of interrogation to quantify the degree of obstruction. TEE imaging, color mapping, and Doppler interrogation should also exclude other associations such as subvalvar AS (ME 4 Ch, ME AV LAX views), an abnormal AoV (ME AV SAX, ME AV LAX views), and coronary artery dilation and coronary ostial obstruction (ME AV SAX, ME AV LAX views). Evaluation of possible coronary ostial obstruction is best performed with color mapping looking for turbulence in the area of stenosis [61–63]. The TG Mid and Basal SAX views can also be used to evaluate for segmental wall motion abnormalities, supporting the possibility of coronary artery obstruction. The branch pulmonary arteries should also be evaluated for possible stenosis using the mid esophageal ascending aorta short axis (ME Asc Ao SAX), upper esophageal pulmonary artery LAX (UE PA LAX), and UE Ao Arch SAX views. The branch pulmonary arteries can be difficult to evaluate by TEE, though color mapping can be quite helpful in ascertaining the presence and location of the stenosis (Chaps. 4 and 13).

Aortic Regurgitation

Isolated congenital AR, defined loosely as diastolic flow from the aortic root into the LV, is a rare lesion [64]. Congenital etiologies causing AR in childhood include a bicuspid or quadricuspid AoV (Fig. 11.15, Video 11.15), a dysplastic tricuspid AoV, an aortico-left ventricular tunnel, absence of one or more AoV leaflets, a coronary-cameral fistula into the LV, and a ruptured sinus of Valsalva aneurysm into the LV. Occasionally AR occurs in the setting of subvalvar AS (as discussed previously), AoV prolapse into a membranous or doubly-committed subarterial VSD, or a ruptured sinus of Valsalva aneurysm into the right atrium (Fig. 11.16, Video 11.16a and 11.16b) or RV. It can also be seen with aortic root dilation in association with neonatal Marfan syndrome, tetralogy of Fallot, or truncus arteriosus.

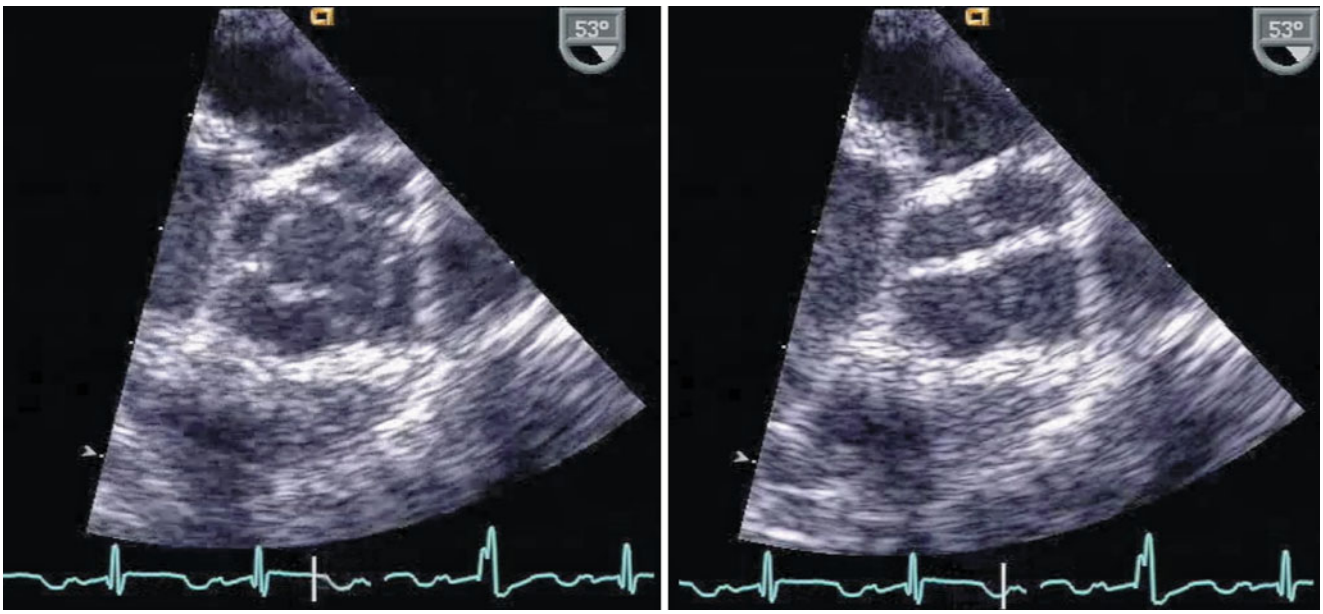

Fig. 11.15 Quadricuspid aortic valve as seen from the mid esophageal aortic valve short axis view, in systole (*left figure*) and diastole (*right figure*)

Acquired AR generally occurs with endocarditis, rheumatic fever, or after surgical or transcatheter balloon valvotomy for valvar AS. AR is a progressive disease. The increased volume load on the LV initially results in compensatory hypertrophy, though the degree of hypertrophy becomes inadequate as regurgitation worsens (decompensated AR). Increasing LV volume associated with decreasing ventricular wall thickness results in increased afterload; eventually this increased afterload leads to myocardial damage and diminished contractility. In an effort to prevent irreversible myocardial damage, some echocardiographic guidelines have been established regarding the timing for intervention. In 2006, the ACC/AHA Task Force on Practice Guidelines recommended an end-diastolic diameter of 75 mm and an end-systolic diameter of 55 mm (as measured in transthoracic parasternal short axis views of the LV) as thresholds for intervention in asymptomatic adults with significant AR [65]. Comparable guidelines for the pediatric population have not yet been established.

The utility of transthoracic echocardiography in assessing the degree of AR and the appropriate timing for intervention has been discussed extensively [66]. Once a patient is in the operating room, TEE provides a highly accurate assessment of all types of AR lesions, whether it is annular dilation, leaflet prolapse (in the setting of a VSD), or leaflet deficiency as in a bicommissural aortic valve or in rheumatic heart disease [67]. This is especially important if surgical repair of the valve is a consideration as valves with bicommissural morphology and those after rheumatic fever tend to be better candidates for surgical repair [68]. Therefore, TEE should evaluate the AoV and aortic root morphology in multiple mid esophageal views. The ME AV SAX view at 30–45° will display abnormalities in AoV commissural morphology, discrepancies among the individual leaflet sizes, absence of one or more of the leaflets, dilation of a coronary artery in the setting of a significant coronary-cameral fistula into the LV, disruption of one or more AoV leaflets (flail segment) secondary to endocarditis or after valvotomy, or rupture of a sinus of Valsalva into one of the intracardiac chambers (Fig. 11.16a, Video 11.16a). The ME AV LAX view at ~120° and ME RV In-Out view between 60° and 90° will display abnormally thickened AoV leaflets after rheumatic fever, an aortico-left ventricular tunnel, or a ruptured sinus of Valsalva aneurysm (Fig. 11.16b, Video 11.16b). The location of the regurgitant jet should be assessed from multiple TEE windows, including the mid esophageal (ME AV SAX, ME AV LAX, ME LAX), deep transgastric (DTG LAX, DTG Sagittal), and transgastric (TG LAX) views. Regarding assessment of AR severity, a 2003 report from the American Society of Echocardiography task force on valvular regurgitation suggested that a vena contracta width for the regurgitant jet >0.6 cm and a ratio between the color flow jet width and the LVOT diameter >65 % represent severe AR [69]. Both of these measurements are best obtained from the ME AV LAX view. In keeping with these recommendations, the 2008 ACC/AHA task force [21] listed the following echocardiographic criteria for classification of AR:

- Mild: Vena contracta width <0.3 cm, jet width/LVOT diameter <25 %
- Moderate: Vena contracta width 0.3–0.6 cm, jet width/LVOT diameter 25–65 %

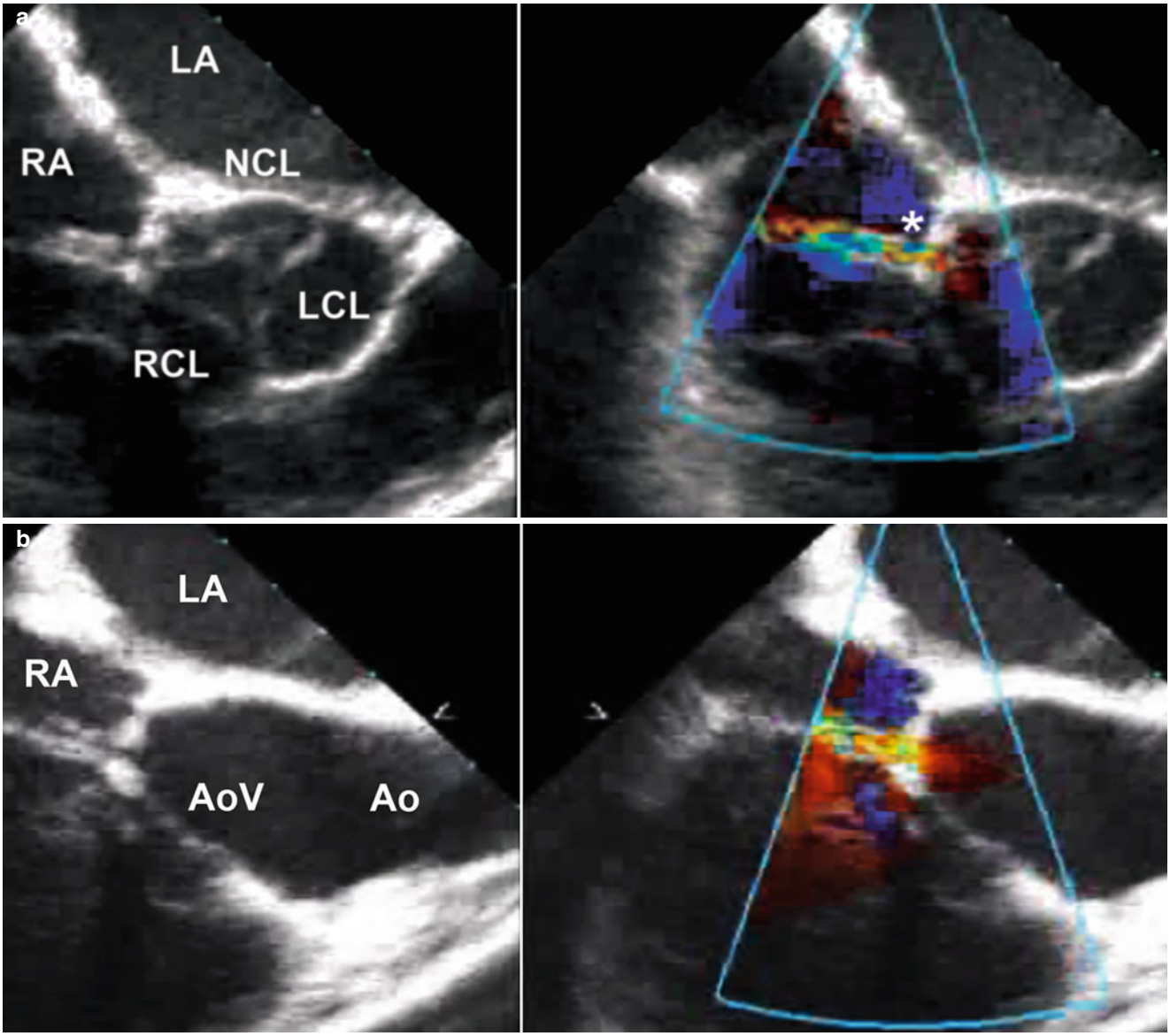

Fig. 11.16 (**a**) Mid esophageal aortic valve short axis view at 45° showing a short axis view of the aortic valve and a ruptured non-coronary sinus of Valsalva aneurysm (*asterisk*) into the right atrium; (**b**) Modified mid esophageal right ventricular inflow-outflow view at 90° showing the same ruptured of sinus of Valsalva aneurysm into the right atrium (*Ao* aorta, *AoV* aortic valve, *LA* left atrium, *LCL* left coronary leaflet, *NCL* non-coronary leaflet, *RA* right atrium, *RCL* right coronary leaflet)

- Severe: Vena contracta width >0.6 cm, jet width/LVOT diameter >65 %.

Other supportive data that can indicate at least moderate AR include prominent retrograde diastolic flow in the descending aorta, as noted by both color flow and pulsed wave Doppler [19, 20, 70]. This can best be evaluated using a combination of upper esophageal (UE Ao Arch LAX, SAX) and descending aorta long axis (Desc Ao LAX) and descending aortic short axis (Desc Ao SAX) views. There are few data on the utility of TEE to evaluate other indices of AR severity such as pressure half-time (which reflects the rate of equalization of aortic and LV diastolic pressures in the setting of AR), especially since this index can be affected by LV compliance, LV diastolic pressures, aortic compliance, and any therapy which changes ventricular afterload [70, 71]. In general, a pressure half-time > 500 ms is usually compatible with mild AR, while a value < 200 ms is consistent with severe AR [69]. Methods that have been discussed in other sources, but are rather difficult and time-consuming to perform in the intraoperative setting, include the calculation of effective regurgitant orifice area (EROA) by the flow convergence method (PISA) [69, 72]. If used, the following grading system (EROA in cm^2) has been suggested: mild AR <0.10, moderate AR 0.10–0.30 severe AR >0.30 [21]. It should be noted that the degree of AR can be difficult to assess by TEE, particularly in the operating room in which

changing hemodynamics and general anesthesia could artificially alter its severity. However, in a cohort of pediatric patients who had undergone aortic valve repair, Honjo *et al*. found that, using the jet width/LVOT criteria, there was reasonable agreement between the degree of AR found by intraoperative TEE and subsequently by pre-discharge transthoracic echocardiogram [73].

In addition to the evaluation of AR, LV size and function should be assessed qualitatively in the transgastric short axis views (TG Mid SAX, TG Basal SAX) at 0°. Associated abnormalities such as subvalvar AS, a VSD, and aortic dilation can be assessed in multiple views as discussed above.

Surgical intervention generally involves aortic valvuloplasty (occasionally involving the use of autologous pericardium), a Ross procedure (involving replacement of the aortic root with the patient's pulmonary root and placement of a homograft from the RV to the pulmonary artery), or AoV replacement with a mechanical valve, bioprosthesis, or homograft valve. The postoperative TEE should exclude residual LVOT obstruction using the transgastric LAX and deep transgastric views: DTG LAX at 0–30°, and DTG Sagittal view at ~90°. Residual AR can be evaluated in multiple mid esophageal, transgastric, and deep transgastric views. After aortic valvuloplasty, a maximum instantaneous gradient >45 mmHg or degree of AR ≥ moderate are considered indications to return to cardiopulmonary bypass for a repeat AoV repair or replacement [74]. After a Ross procedure, any neo-AR is a highly sensitive predictor of ≥ moderate neo-AR at the time of hospital discharge [75] If a prosthetic aortic valve is present, symmetric motion of the valve leaflets can usually be seen in the mid esophageal views, particularly the ME AV SAX and ME AV LAX views (Fig. 11.17, Video 11.17), though this can become difficult secondary to acoustic interference from the prosthetic valve annular ring. The transgastric and deep transgastric views are helpful here: since they visualize the valve from the left ventricular aspect, they avoid shadowing and reverberation artifacts, allowing evaluation of the "upstream" portion of the prosthetic valve and leaflet motion. Doppler evaluation of the prosthetic valve should be performed from the transgastric or deep transgastric views, as described above and discussed in Chap. 16.

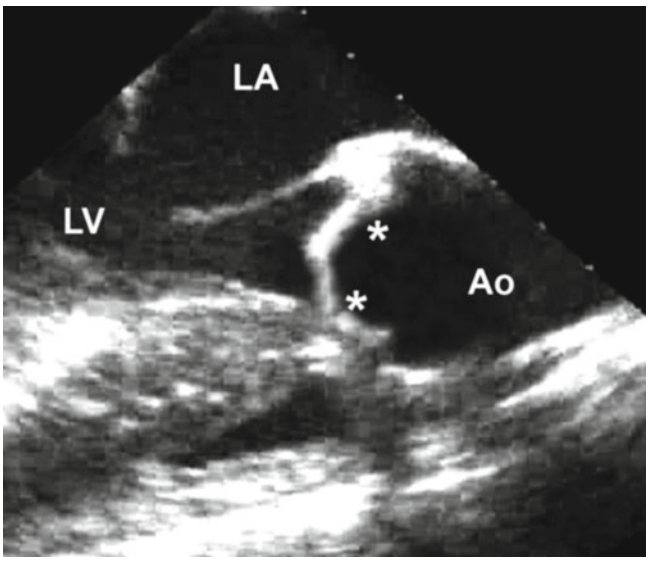

Fig. 11.17 Mid esophageal aortic valve long axis view at 120° showing a prosthetic aortic valve with symmetric positioning of the prosthetic hemidisc leaflets (*asterisks*) (*Ao* aorta, *LA* left atrium, *LV* left ventricle)

Aneurysm of the Proximal Aorta

Formation of an aortic root aneurysm and aneurysmal dilation of the proximal aorta result from an intrinsic aortopathy, usually involving smooth muscle cell loss and extracellular matrix disruption (cystic medial necrosis). These structural abnormalities in the muscular and elastic components lead to thinned and weakened aortic walls. As seen in supravalvar AS, abnormalities in elastin homeostasis may play a major role in the development of aortic root aneurysms and a dilated proximal aorta. For example, Marfan syndrome, with its predilection for aortic root dilation, is caused by mutations in the fibrillin gene on chromosome 15 [76], and fibrillin is an important glycoprotein necessary for elastin production and maintenance [77]. Associations with dilation of the proximal aorta include Marfan syndrome, Loeys-Dietz syndrome, Ehlers-Danlos syndrome, Turner syndrome, a bicuspid AoV, systemic hypertension, and aortic coarctation. Congenital cardiac defects known to be associated include tetralogy of Fallot, D-transposition of the great arteries, and truncus arteriosus [78]. Because of the intrinsic weakness in the aortic wall, a sinus of Valsalva aneurysm is at risk for rupture into the right and left heart chambers (most frequently into the RV) [79] (Fig. 11.16, Video 11.16a and 11.16b), and a dilated aortic root or ascending aorta is at risk for dissection and rupture [80] (Fig. 11.18, Video 11.18). Both of these problems are frequently associated with AR [79, 81]. In addition, aortic root aneurysms are also frequently associated with a VSD [79]. TEE is frequently superior to transthoracic echocardiography in the evaluation of the entire extent of the proximal aorta, particularly in older children and in adults, and occasionally a TEE study is performed before the decision to intervene surgically is made. Mid esophageal views at multiple angles can display a sinus of Valsalva aneurysm as well as its spatial relationship to surrounding cardiac structures. Color mapping can easily display the continuous restrictive jet of a ruptured aneurysm into the right atrium, RV, and left atrium; when the aneurysm ruptures into the LV, color mapping can display the diastolic jet. The location and degree of AR can also be evaluated with color mapping in multiple mid esophageal views.

Aneurysmal dilation of the aortic root and ascending aorta is best evaluated with ME AV LAX and ME Asc Ao LAX views between 90° and 130° (Fig. 11.19, Video 11.19). One should always look for the characteristic parallel lines of dissection along the aortic wall in these patients from multiple mid esophageal views (Fig. 11.18, Video 11.18), and color mapping will occasionally show the connection between the dissection and the aortic lumen. The more superior portion of the ascending aorta, as well as aortic arch and proximal descending aorta, can also be evaluated for dilation and possible dissection using the upper esophageal TEE views (UE Ao Arch LAX at 90–120°, UE Ao Arch SAX at 0°). See Chap. 16 for further discussion on the TEE evaluation of aortic dissection.

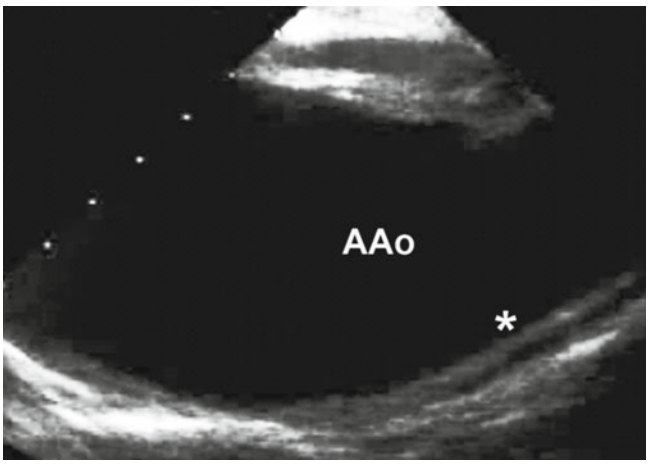

Fig. 11.18 Mid esophageal ascending aortic long axis view at 120° showing a markedly dilated aortic root and ascending aorta with associated aortic dissection along the anterior wall of the ascending aorta (the double linear density representing the aortic dissection along the anterior ascending aortic wall is indicated by the *asterisk*) in a patient with Marfan syndrome (*AAo* ascending aorta)

Right Ventricular Outflow Tract Anomalies

Valvar Pulmonary Stenosis

Valvar PS is one of the most commonly occurring types of congenital heart disease [1, 2]. It can present either as thin but doming leaflets with tricuspid or bicuspid morphology or as dysplastic leaflets with thickened edges. The former represents the more common presentation and is often associated with post-stenotic dilation of the main pulmonary trunk (Fig. 11.20, Video 11.20). Because one or more of the commissures can be partially or completely fused or underdeveloped (with formation of a raphé), the thickened raphé can appear tethered to the arterial wall at the sino-tubular junction, giving the lesion the appearance of supravalvar narrowing (Fig. 11.20, Video 11.20). As discussed previously, the semilunar valve attachments extend up to the sino-tubular junction [82] (Fig. 11.3b), and this particular variant of valvar PS can sometimes be difficult to distinguish from discrete narrowing of the pulmonary sino-tubular junction (supravalvar stenosis) without valvar obstruction. Because of the underdeveloped distal segments of the commissures, the leaflets are often attached in a more circular fashion at the pulmonary root rather than the normal semilunar arrangement discussed previously [83]. The dysplastic form of valvar PS is not as common and is often associated with pulmonary annular hypoplasia and a small pulmonary trunk. The leaflets are usually attached to the pulmonary root in a semilunar fashion. Occasionally there is separate but discrete narrowing of the pulmonary sino-tubular junction resulting in combined valvar and supravalvar PS. Valvar PS places excess pressure load on the RV, often resulting in significant RV hypertrophy, which in turn can contribute to the total obstruction along the RVOT. An atrial septal defect or patent foramen ovale is also commonly found in these patients [84].

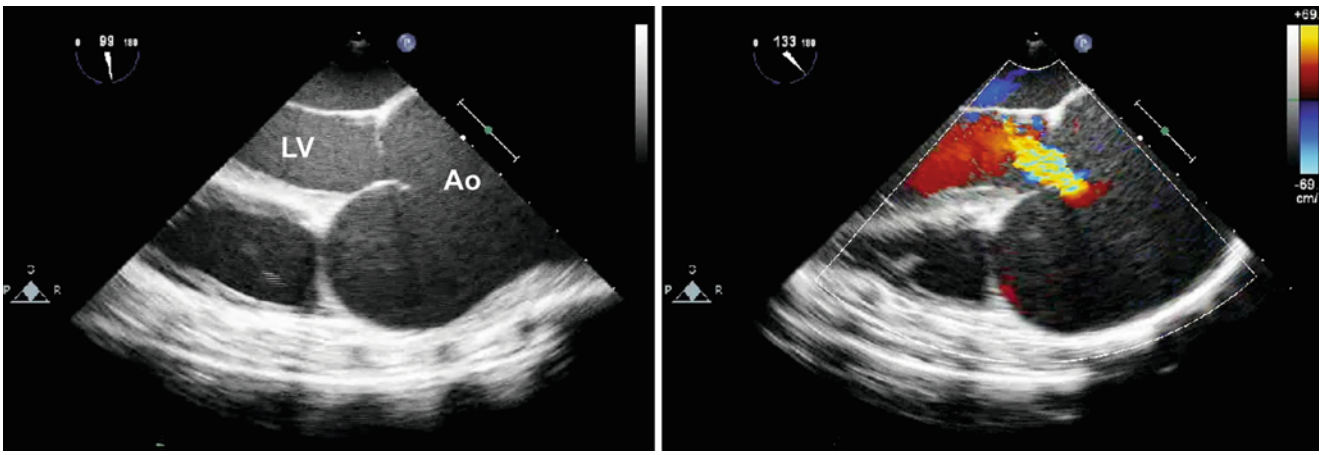

Fig. 11.19 Markedly dilated aortic root as seen from the mid esophageal aortic valve long axis view without color mapping (*left panel*) and with color mapping, showing central aortic regurgitation (*right panel*). *Ao* aorta, *LV* left ventricle

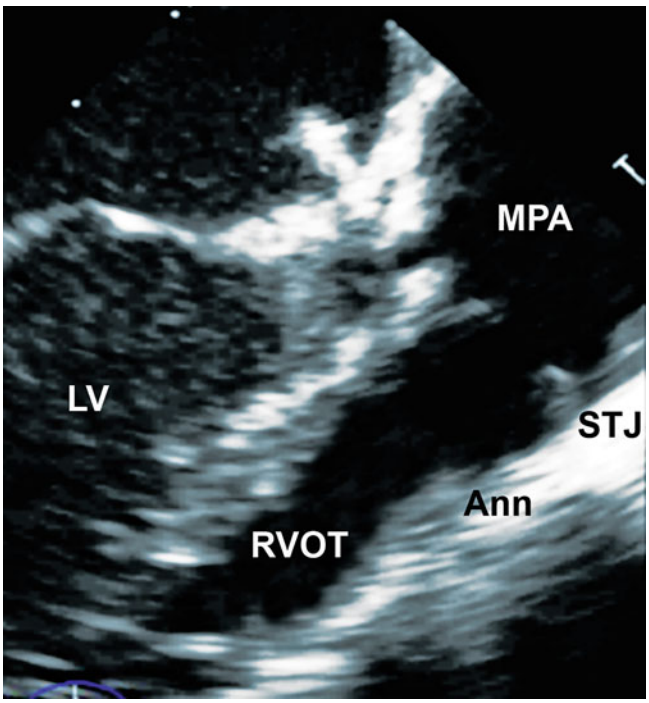

Fig. 11.20 Mid esophageal aortic valve long axis view with multiplane angle at 90° and slight leftward probe rotation. This image shows valvar pulmonary stenosis with thin but doming pulmonary valve leaflets abutting against the sino-tubular junction and post-stenotic dilation of the main pulmonary artery (*Ann* pulmonary annulus, *LV* left ventricle, *MPA* main pulmonary artery, *RVOT* right ventricular outflow tract, *STJ* pulmonary sino-tubular junction)

Because the majority of these patients undergo intervention when necessary in the catheterization laboratory, TEE is rarely needed to evaluate the pulmonary valve morphology and degree of obstruction. However, TEE is frequently used during transcatheter device closure of atrial septal defects, and the excess pulmonary blood flow associated with these lesions often results in turbulence across the pulmonary valve without true valvar PS (relative PS). TEE performed in the catheterization laboratory can help determine whether intervention is necessary at the pulmonary valve. The RVOT, and particularly the pulmonary valve, can easily be evaluated with the ME AV SAX at 0°, the ME RV In-Out view at 60°–90°, and a modified ME AV LAX at 90° with leftward probe rotation to visualize the pulmonary outflow tract (Fig. 11.20, Video 11.20). Occasionally, a higher esophageal view, such as ME Asc Ao SAX or upper esophageal view (UE PA LAX at 0°, UE Ao Arch SAX at 90°), is necessary in patients with an elongated subpulmonary conus. Quantitative assessment of the degree of valvar PS can be performed in the DTG Sagittal view at 90° (Fig. 11.1b, Video 11.1b) in the same way that LVOT obstruction is evaluated by Doppler interrogation, usually requiring slight rotation of the probe to visualize the RVOT. Occasionally, the degree of valvar PS can be assessed in ME Asc Ao SAX and UE PA LAX view at 0° by interrogating the high velocity flow into the main pulmonary trunk (Figs. 11.21 and 11.22; Video 11.21). This view also allows for measurements of the main and proximal branch

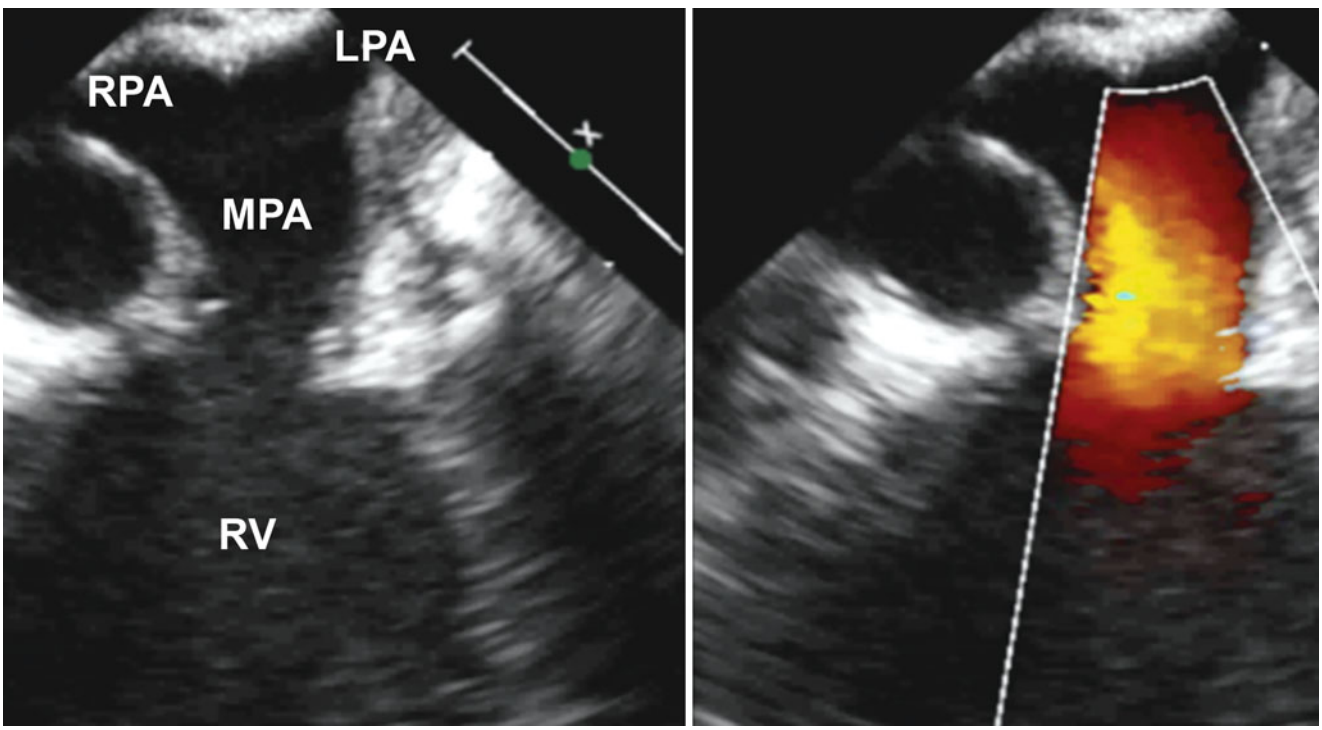

Fig. 11.21 Upper esophageal pulmonary artery long axis view at 0° showing the main pulmonary artery in the setting of mild valvar pulmonary stenosis with thin doming pulmonary valve leaflets, and minimal flow acceleration across the valve. In this image the bifurcation of the branch pulmonary arteries can also be seen (*LPA* left pulmonary artery, *MPA* main pulmonary artery, *RPA* right pulmonary artery, *RV* right ventricle)

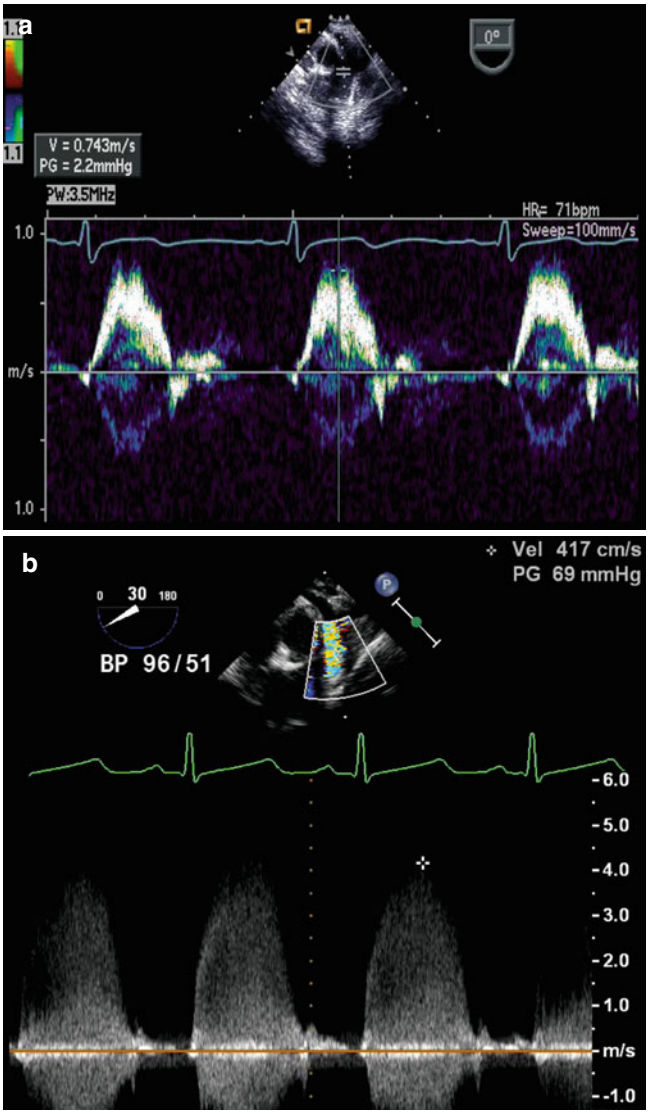

Fig. 11.22 Spectral Doppler recordings of flow across the pulmonary valve, as obtained from the mid esophageal ascending aortic short axis view at 0°. In (**a**), there is normal, low velocity laminar flow seen in the main pulmonary artery through a normal pulmonary valve. In (**b**), high velocity flow is obtained by continuous wave Doppler across a pulmonary valve that is stenotic

pulmonary artery diameters. In many instances, the UE PA LAX and UE Ao Arch SAX views provide an excellent angle for Doppler interrogation of the high velocity jet arising from the pulmonary valve (Video 11.20).

There are a number of congenital heart defects in which pulmonary stenosis (subvalvar, valvar, and sometimes supravalvar) is a frequent finding. At times, pulmonary outflow obstruction is an important and integral part of the anatomic spectrum of the cardiac defect. Examples of such anomalies include tetralogy of Fallot, double outlet right ventricle, tricuspid atresia, and transposition of the great arteries, and these cardiac defects are discussed in other chapters in this textbook. Nonetheless, the TEE evaluation of the pulmonary outflow tract in those conditions mirrors that described in this chapter and should be performed using a similar approach.

Subvalvar Pulmonary Stenosis (Double-Chambered Right Ventricle)

A double-chambered RV (DCRV) is a type of RVOT obstruction involving anomalously prominent RV muscle bundles that divide the RV into two chambers: a proximal high-pressure inflow chamber and a distal low-pressure outflow chamber (Fig. 11.23, Video 11.22). Some prefer to use the term divided RV for this lesion [85], although a divided RV does not always involve anomalous RV muscle bundles [86]. The division in a DCRV usually occurs at the infundibular os, with the distal outflow chamber corresponding to a well-developed subpulmonary infundibulum. Like subvalvar AS, the obstruction associated with a DCRV is not always present early in life, prompting some people to classify the lesion as an acquired disease [87]. However, others suggest that a congenital anatomic substrate for a DCRV is present before obstruction develops and can actually be predicted echocardiographically by measuring the distance from the moderator band to the PV [88]. In this setting, DCRV is thought to result from superior displacement and hypertrophy of the moderator band, contributing to progressive obstruction at the infundibular os. Others suggest, however, that the anomalously prominent muscle bundles in a DCRV are in fact distinct from the moderator band since the septal attachment of a normal moderator band is located more apically than the usual attachments of these anomalous muscle bundles [89]. The most common association is a VSD, usually a small or moderate membranous VSD, occurring in at least 67 % of these patients [90]. Viewed in another manner, a DCRV can be present in up to 10 % of patients who require VSD surgery [91], necessitating careful assessment of the RVOT in all patients with a VSD. Another common association is a fixed subaortic ridge or echo dense area at the crest of the ventricular septum, occurring in up to 88 % of patients with a DCRV and a VSD, although some degree of subvalvar AS is present in only a quarter of these patients [49]. This lesion must be distinguished from tetralogy of Fallot, wherein anterior and superior deviation of the conal septum results in a large VSD and an underdeveloped subpulmonary infundibulum.

The RVOT obstruction in DCRV is usually progressive, presenting during childhood or adolescence, although cases of adult presentation have been reported [90, 92]. Almost all cases require surgical intervention. TEE is useful in the preoperative evaluation, and the infundibular os and RVOT are easily visualized in the ME RV In-Out view with multiplane angle between 60° and 90°. However, the anterior location of

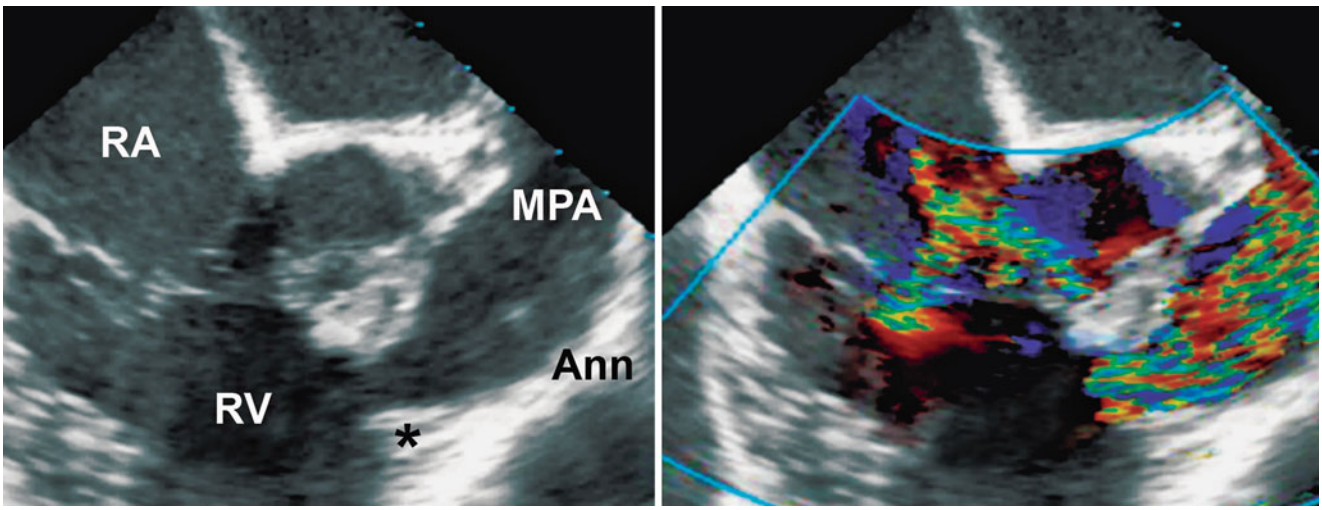

Fig. 11.23 Mid esophageal right ventricular inflow-outflow view at 60° showing a double-chambered right ventricle with prominent muscle bundles at the infundibular os (*asterisk*) separating the proximal right ventricular chamber from the well-developed right ventricular infundibular chamber and resulting in subvalvar pulmonary stenosis (the pulmonary annulus is within normal limits in size). (Moderate tricuspid regurgitation is also present *Ann* pulmonary annulus, *MPA* main pulmonary artery, *RA* right atrium, *RV* right ventricle)

the prominent muscle bundles and their proximity to the probe often makes qualitative assessment of the extent of the muscle bundles difficult. Thus this area should be examined carefully as it is easy to overlook RVOT obstruction at this level. In addition, the orientation of blood flow across the muscle bundles is often directly perpendicular to the echocardiographic beam in the mid esophageal views, precluding adequate color mapping and quantitative spectral Doppler interrogation of the area (Fig. 11.23, Video 11.22). Quantitative assessment of the degree of RVOT obstruction is best performed in the DTG Sagittal view at 90° as discussed in the previous section (Fig. 11.24, Video 11.23). Postoperative evaluation after resection of the muscle bundles should exclude residual obstruction in the DTG Sagittal view at 90°; the TEE study should evaluate for the development of pulmonary regurgitation in multiple mid esophageal views. Occasionally, resection of the muscle bundles results in the development of tiny coronary-cameral fistulae along the RV anterior free wall, and these are easily visualized with color mapping in multiple mid esophageal views.

Pulmonary Regurgitation

Pulmonary regurgitation (PR) is a common finding during routine echocardiographic evaluation with a prevalence of up to 88 % in normal healthy children and up to 68 % in healthy adults [93]. The prevalence may decrease later in adulthood, though this trend may be more related to technical limitations in adults with poor echocardiographic windows rather than a true decrease in the frequency of the lesion. Among the 3,370 subjects with pulmonary outflow tract anomalies evaluated by echocardiography at Children's Hospital Boston from 1988 to 2002, over 40 % (1403) had PR and almost 24 % of these (335) had ≤ mild PR without associated cardiac structural abnormalities [94]. Isolated PR as a congenital anomaly is extremely rare and has been associated with aneurysmal dilation of the pulmonary arteries secondary to cystic medial necrosis (as seen in the aortopathy of Marfan syndrome and bicuspid AoV) [95]. Many of these patients do not require intervention, unless the severity of the PR results in significant RV dilation and dysfunction. Occasionally, isolated PR with idiopathic dilation of the pulmonary arteries is associated with absence of one or more PV leaflets [95, 96]. Although this is seen more frequently in the setting of tetralogy of Fallot with absent or dysplastic PV leaflets, it can occur as an isolated abnormality, and marked dilation of the pulmonary arteries can also occur, resulting in significant airway compression that requires surgical intervention.

Quantification of PR is not as well established by echocardiography (either transthoracic or transesophageal). Doppler methods, both color flow and spectral, are generally used, though variable hemodynamic conditions (RV diastolic properties and filling pressures, driving pressure between pulmonary artery and RV, etc.) will influence the Doppler evaluation. Pulsed wave Doppler assessment of the forward and reverse flow in the main pulmonary artery (using the velocity time integral) could theoretically be used to estimate the percent and volume of regurgitant flow; however this method has not been standardized and also is not valid in patients with pulmonary valve stenosis. Criteria for vena contracta width (which would seem to be more accurate than jet width) and regurgitant orifice area width to assess PR

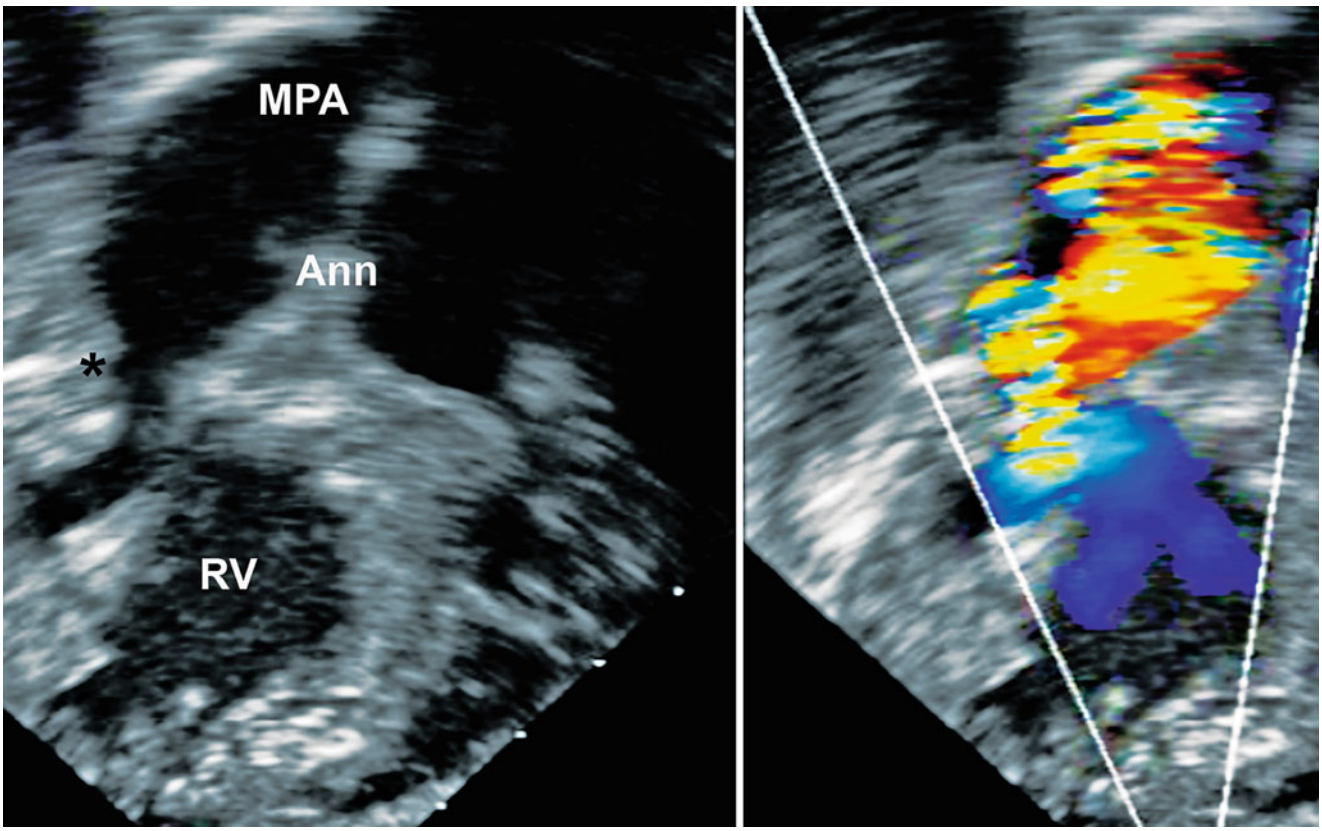

Fig. 11.24 Deep transgastric sagittal view at 90° showing a double-chambered right ventricle with prominent muscle bundles at the infundibular os (*asterisk*) separating the proximal right ventricular chamber from the well-developed right ventricular infundibular chamber and resulting in subvalvar pulmonary stenosis (the pulmonary annulus is within normal limits in size); this is an ideal view to measure the gradient along the right ventricular outflow tract (*Ann* pulmonary annulus, *MPA* main pulmonary artery, *RV* right ventricle)

Table 11.1 Echocardiographic and Doppler parameters used in grading pulmonary regurgitation severity

Parameter	Mild	Moderate	Severe
Pulmonary valve	Normal	Normal or abnormal	Abnormal
RV size	Normal[a]	Normal or dilated	Dilated
Jet size by color flow Doppler[b]	Thin (usually <10 mm in length) with a narrow origin	Intermediate	Usually large, with a wide origin; may be brief in duration
Jet density and deceleration rate—CW[c]	Soft; slow deceleration	Dense; variable deceleration	Dense; steep deceleration, early termination of diastolic flow
Pulmonic systolic flow compared to systemic flow—PW[d]	Slightly increased	Intermediate	Greatly increased

Reprinted from Zoghbi et al [69]; with permission from Elsevier
CW continuous wave Doppler, *PR* pulmonic regurgitation, *PW* pulsed wave Doppler, *RA* right atrium, *RF* regurgitant fraction, *RV* right ventricle
[a]Unless there are other reasons for RV enlargement
[b]At a Nyquist limit of 50–60 cm/s
[c]Steep deceleration is not specific for severe PR
[d]Cut-off values for regurgitant volume and fraction are not well validated

severity have not been well established [70]. Indirect evidence of PR severity can be obtained by evaluating RV size and function, though with by echocardiography this can be more challenging due to the more complex shape of the RV. Also, the RV diastolic properties (specifically the stiffness) can affect the degree of RV dilation. Some of the features commonly used to grade PR severity are listed in Table 11.1 [73]. Overall, it is clear that the grading of PR severity is more difficult because standards for its quantification are less well defined than for AR [70, 97]. Thus when assessing severity of PR, an integrated approach is probably best, utilizing color flow Doppler, continuous and pulsed wave spectral Doppler, as well as evaluations of the pulmonary valve and RV sizes and RV function [73].

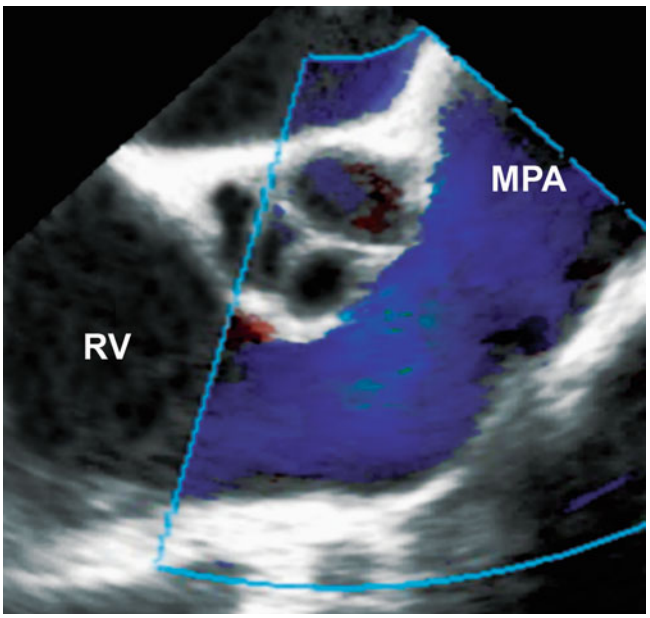

Fig. 11.25 Mid esophageal right ventricular inflow-outflow view at 60° showing free pulmonary regurgitation in the setting of tetralogy of Fallot repair with a transannular right ventricular outflow tract patch (*MPA* main pulmonary artery, *RV* right ventricle)

The most common scenarios for significant PR occur after some type of intervention: after surgical repair of tetralogy of Fallot (Fig. 11.25, Video 11.24), after surgical or transcatheter balloon valvotomy for valvar PS, and after surgical placement of a homograft from the RV to the pulmonary artery for lesions such as tetralogy of Fallot (with or without pulmonary atresia), truncus arteriosus, transposition of the great arteries with a VSD, and pulmonary atresia with intact ventricular septum. As in patients with significant AR, significant PR is associated initially with an increase in RV end-diastolic volume, followed by an increase in RV end-systolic volume, followed by a decrease in RV function and contractility. Symptoms of right-sided heart failure appear, signaling the development of irreversible RV myocardial damage. In many postoperative instances, there are markedly akinetic segments of the RV due to outflow tract patch augmentation and aggressive muscular resection, contributing to the progressive RV systolic and diastolic dysfunction. In addition, newly acquired, significant postoperative PR is not well tolerated by older patients, unlike neonates and children who respond better to this postoperative problem. Strategies for timing of intervention in these patients necessarily involves echocardiographic evaluation, and some of the echocardiographic indices for PR include pressure half-time of the regurgitant jet, presence of flow reversal in the branch pulmonary arteries, and RV size and function [98]. Other echocardiographic indicators are listed above. Restrictive RV physiology can also be identified when diastolic forward flow is seen in the main pulmonary artery during atrial systole by Doppler interrogation [99]. More recently, magnetic resonance imaging and its ability to quantitatively assess RV size and function have superseded echocardiography in determining the timing of intervention [100–102].

Intraoperative assessment of PR by TEE involves color mapping in mid esophageal views along multiple planes such as the ME AV SAX and ME RV In-Out views (Fig. 11.25, Video 11.24). Occasionally a somewhat higher esophageal view, such as the ME Asc Ao SAX and upper esophageal views (UE PA LAX, UE Ao Arch SAX), can provide better color mapping display of the to-and-fro flow across the PV; these views can also display diastolic reversal in the proximal branch pulmonary arteries by color mapping and pulsed wave Doppler interrogation. The DTG Sagittal view of the RVOT at 90° can also display the PR, especially since the direction of flow is parallel to the echocardiographic beam. However, the distance from the probe to the RVOT often limits color mapping in this view for larger patients. Following implantation of a PV, the postoperative TEE examination should exclude residual PR in multiple mid esophageal views and in the DTG Sagittal view at 90°. The new PV, whether it is a mechanical prosthetic valve, a bioprosthetic valve, or part of a valved homograft, should also be evaluated in mid esophageal views using multiple planes such as the ME RV In-Out and MV AV LAX with slight leftward rotation of the probe. The deep transgastric views (DTG Sagittal and LAX) can also be useful in evaluating the flow across the pulmonary valve, both with color flow and spectral Doppler.

Summary

This chapter discusses the common congenital defects affecting the right and left ventricular outflow tracts in both children and adults. While the semilunar valves are most commonly involved, pathology can be seen at any level—subvalvar, valvar, supravalvar, or a combination of one or more levels. Stenosis and/or regurgitation at either or both outflow tracts can occur. Thus a careful echocardiographic evaluation must be undertaken to define precisely the nature, location, and severity of the abnormality/abnormalities. For evaluation of the outflow tracts, TEE excels by providing excellent anatomic imaging and color mapping. It plays a vital role in the perioperative evaluation of outflow tract abnormalities with precise characterization of the pathology preoperatively and assessment of the adequacy of surgical repair postoperatively. It is also important in the evaluation of interventional procedures such as TAVR/TAVI. In addition, TEE can also be valuable in the ambulatory setting, such as the evaluation of subaortic stenosis in older patients. Thus for the assessment and treatment of outflow tract abnormalities, TEE serves as an important and extremely valuable tool.

References

1. Hoffman JI, Kaplan S. The incidence of congenital heart disease. J Am Coll Cardiol. 2002;39:1890–900.
2. Triedman JK. Methodological issues for database development: trends. In: Keane JF, Fyler DC, Lock J, editors. Nadas' pediatric cardiology. 2nd ed. Philadelphia: Saunders; 2006. p. 323–36.
3. Campbell M. Calcific aortic stenosis and congenital bicuspid aortic valves. Br Heart J. 1968;30:606–16.
4. Roberts WC. The congenitally bicuspid aortic valve. A study of 85 autopsy cases. Am J Cardiol. 1970;26:72–83.
5. Ward C. Clinical significance of the bicuspid aortic valve. Heart. 2000;83:81–5.
6. Shanewise JS, Cheung AT, Aronson S, et al. ASE/SCA guidelines for performing a comprehensive intraoperative multiplane transesophageal echocardiography examination: recommendations of the American Society of Echocardiography Council for Intraoperative Echocardiography and the Society of Cardiovascular Anesthesiologists Task Force for Certification in Perioperative Transesophageal Echocardiography. J Am Soc Echocardiogr. 1999;12:884–900.
7. Anderson RH, Freedom RM. Normal and abnormal structure of the ventriculo-arterial junctions. Cardiol Young. 2005;15 Suppl 1:3–16.
8. Dare AJ, Veinot JP, Edwards WD, Tazelaar HD, Schaff HV. New observations on the etiology of aortic valve disease: a surgical pathologic study of 236 cases from 1990. Hum Pathol. 1993;24:1330–8.
9. Angelini A, Ho SY, Anderson RH, et al. The morphology of the normal aortic valve as compared with the aortic valve having two leaflets. J Thorac Cardiovasc Surg. 1989;98:362–7.
10. Fernandes SM, Sanders SP, Khairy P, et al. Morphology of bicuspid aortic valve in children and adolescents. J Am Coll Cardiol. 2004;44:1648–51.
11. Beppu S, Suzuki S, Matsuda H, Ohmori F, Nagata S, Miyatake K. Rapidity of progression of aortic stenosis in patients with congenital bicuspid aortic valves. Am J Cardiol. 1993;71:322–7.
12. Fernandes SM, Khairy P, Sanders SP, Colan SD. Bicuspid aortic valve morphology and interventions in the young. J Am Coll Cardiol. 2007;49:2211–4.
13. Miller MJ, Geffner ME, Lippe BM, et al. Echocardiography reveals a high incidence of bicuspid aortic valve in Turner syndrome. J Pediatr. 1983;102:47–50.
14. Fedak PW, Verma S, David TE, Leask RL, Weisel RD, Butany J. Clinical and pathophysiological implications of a bicuspid aortic valve. Circulation. 2002;106:900–4.
15. Nistri S, Sorbo MD, Basso C, Thiene G. Bicuspid aortic valve: abnormal aortic elastic properties. J Heart Valve Dis. 2002;11:369–73; discussion 373–4.
16. Nkomo VT, Enriquez-Sarano M, Ammash NM, et al. Bicuspid aortic valve associated with aortic dilatation: a community-based study. Arterioscler Thromb Vasc Biol. 2003;23:351–6.
17. Wagner HR, Ellison RC, Keane JF, Humphries OJ, Nadas AS. Clinical course in aortic stenosis. Circulation. 1977;56:I47–56.
18. Keane JF, Driscoll DJ, Gersony WM, et al. Second natural history study of congenital heart defects. Results of treatment of patients with aortic valvar stenosis. Circulation. 1993;87:I16–27.
19. Mehta Y, Singh R. Quantification of AS and AR. Ann Card Anaesth. 2009;12:166.
20. Savino JS. Transesophageal echocardiographic evaluation of native valvular disease and repair. Crit Care Clin. 1996;12:321–81.
21. Bonow RO, Carabello BA, Chatterjee K, et al. 2008 Focused update incorporated into the ACC/AHA 2006 guidelines for the management of patients with valvular heart disease: a report of the American College of Cardiology/American Heart Association Task Force on Practice Guidelines (Writing Committee to Revise the 1998 Guidelines for the Management of Patients With Valvular Heart Disease): endorsed by the Society of Cardiovascular Anesthesiologists, Society for Cardiovascular Angiography and Interventions, and Society of Thoracic Surgeons. Circulation. 2008;118:e523–661.
22. Heinrich RS, Fontaine AA, Grimes RY, et al. Experimental analysis of fluid mechanical energy losses in aortic valve stenosis: importance of pressure recovery. Ann Biomed Eng. 1996; 24:685–94.
23. Baumgartner H, Hung J, Bermejo J, et al. Echocardiographic assessment of valve stenosis: EAE/ASE recommendations for clinical practice. Eur J Echocardiogr. 2009;10:1–25.
24. Nakai H, Takeuchi M, Yoshitani H, Kaku K, Haruki N, Otsuji Y. Pitfalls of anatomical aortic valve area measurements using two-dimensional transoesophageal echocardiography and the potential of three-dimensional transoesophageal echocardiography. Eur J Echocardiogr. 2010;11:369–76.
25. Schneider DJ, Moore JW. Aortic stenosis. In: Allen HD, Driscoll DJ, Shaddy RE, Feltes TF, editors. Moss and Adams' heart disease in infants, children, and adolescents: including the fetus and young adult. 7th ed. Philadelphia: Lippincott Williams & Wilkins; 2008. p. 968–87.
26. Simpson JM. Anomalies of left ventricular outflow tract and aortic valve. In: Lai W, Mertens L, Cohen MS, Geva T, editors. Echocardiography in pediatric and congenital heart disease: from fetus to adult. Illustrated Ed. Chichester/Hoboken: Wiley; 2009. p. 297–314.
27. Lopez L. Abnormalities of left ventricular outflow. In: Eidem BW, Ceteta F, O'Leary PW, editors. Echocardiography in pediatric and adult congenital heart disease. Philadelphia: Lippincott Williams & Wilkins; 2010. p. 215–36.
28. Lopez L, Colan SD, Frommelt PC, et al. Recommendations for quantification methods during the performance of a pediatric echocardiogram: a report from the Pediatric Measurements Writing Group of the American Society of Echocardiography Pediatric and Congenital Heart Disease Council. J Am Soc Echocardiogr. 2010;23:465–95.
29. Daubeney PE, Blackstone EH, Weintraub RG, Slavik Z, Scanlon J, Webber SA. Relationship of the dimension of cardiac structures to body size: an echocardiographic study in normal infants and children. Cardiol Young. 1999;9:402–10.
30. Pettersen MD, Du W, Skeens ME, Humes RA. Regression equations for calculation of z scores of cardiac structures in a large cohort of healthy infants, children, and adolescents: an echocardiographic study. J Am Soc Echocardiogr. 2008;21:922–34.
31. Leon MB, Smith CR, Mack M, et al. Transcatheter aortic-valve implantation for aortic stenosis in patients who cannot undergo surgery. N Engl J Med. 2010;363:1597–607.
32. Billings FT, Kodali SK, Shanewise JS. Transcatheter aortic valve implantation: anesthetic considerations. Anesth Analg. 2009;108:1453–62.
33. Webb JG, Wood DA. Current status of transcatheter aortic valve replacement. J Am Coll Cardiol. 2012;60:483–92.
34. Makkar RR, Fontana GP, Jilaihawi H, et al. Transcatheter aortic-valve replacement for inoperable severe aortic stenosis. N Engl J Med. 2012;366:1696–704.
35. Gilard M, Eltchaninoff H, Iung B, et al. Registry of transcatheter aortic-valve implantation in high-risk patients. N Engl J Med. 2012;366:1705–15.
36. Leichter DA, Sullivan I, Gersony WM. "Acquired" discrete subvalvular aortic stenosis: natural history and hemodynamics. J Am Coll Cardiol. 1989;14:1539–44.
37. Vogt J, Dische R, Rupprath G, de Vivie ER, Kotthoff S, Kececioglu D. Fixed subaortic stenosis: an acquired secondary obstruction? A twenty-seven year experience with 168 patients. Thorac Cardiovasc Surg. 1989;37:199–206.
38. Cape EG, Vanauker MD, Sigfusson G, Tacy TA, del Nido PJ. Potential role of mechanical stress in the etiology of pediatric heart disease: septal shear stress in subaortic stenosis. J Am Coll Cardiol. 1997;30:247–54.

39. Cilliers AM, Gewillig M. Rheology of discrete subaortic stenosis. Heart. 2002;88:335–6.
40. Kleinert S, Geva T. Echocardiographic morphometry and geometry of the left ventricular outflow tract in fixed subaortic stenosis. J Am Coll Cardiol. 1993;22:1501–8.
41. Sigfusson G, Tacy TA, Vanauker MD, Cape EG. Abnormalities of the left ventricular outflow tract associated with discrete subaortic stenosis in children: an echocardiographic study. J Am Coll Cardiol. 1997;30:255–9.
42. Bezold LI, Smith EO, Kelly K, Colan SD, Gauvreau K, Geva T. Development and validation of an echocardiographic model for predicting progression of discrete subaortic stenosis in children. Am J Cardiol. 1998;81:314–20.
43. Melero JM, Rodriguez I, Such M, Porras C, Olalla E. Left ventricular outflow tract obstruction with mitral mechanical prosthesis. Ann Thorac Surg. 1999;68:255–7.
44. Rietman GW, van der Maaten JMAA, Douglas YL, Boonstra PW. Echocardiographic diagnosis of left ventricular outflow tract obstruction after mitral valve replacement with subvalvular preservation. Eur J Cardiothorac Surg. 2002;22:825–7.
45. Wu Q, Zhang L, Zhu R. Obstruction of left ventricular outflow tract after mechanical mitral valve replacement. Ann Thorac Surg. 2008;85:1789–91.
46. Geva T, Hornberger LK, Sanders SP, Jonas RA, Ott DA, Colan SD. Echocardiographic predictors of left ventricular outflow tract obstruction after repair of interrupted aortic arch. J Am Coll Cardiol. 1993;22:1953–60.
47. Salem MM, Starnes VA, Wells WJ, et al. Predictors of left ventricular outflow obstruction following single-stage repair of interrupted aortic arch and ventricular septal defect. Am J Cardiol. 2000;86:1044–7.
48. Silverman NH, Gerlis LM, Ho SY, Anderson RH. Fibrous obstruction within the left ventricular outflow tract associated with ventricular septal defect: a pathologic study. J Am Coll Cardiol. 1995;25:475–81.
49. Vogel M, Smallhorn JF, Freedom RM, Coles J, Williams WG, Trusler GA. An echocardiographic study of the association of ventricular septal defect and right ventricular muscle bundles with a fixed subaortic abnormality. Am J Cardiol. 1988;61:857–60.
50. Coleman DM, Smallhorn JF, McCrindle BW, Williams WG, Freedom RM. Postoperative follow-up of fibromuscular subaortic stenosis. J Am Coll Cardiol. 1994;24:1558–64.
51. Oliver JM, Gonzalez A, Gallego P, Sanchez-Recalde A, Benito F, Mesa JM. Discrete subaortic stenosis in adults: increased prevalence and slow rate of progression of the obstruction and aortic regurgitation. J Am Coll Cardiol. 2001;38:835–42.
52. Stassano P, Di Tommaso L, Contaldo A, et al. Discrete subaortic stenosis: long-term prognosis on the progression of the obstruction and of the aortic insufficiency. Thorac Cardiovasc Surg. 2005; 53:23–7.
53. Kuralay E, Ozal E, Bingöl H, Cingöz F, Tatar H. Discrete subaortic stenosis: assessing adequacy of myectomy by transesophageal echocardiography. J Card Surg. 1999;14:348–53.
54. Darcin OT, Yagdi T, Atay Y, et al. Discrete subaortic stenosis: surgical outcomes and follow-up results. Tex Heart Inst J. 2003; 30:286–92.
55. Bernhard WF, Keane JF, Fellows KE, Litwin SB, Gross RE. Progress and problems in the surgical management of congenital aortic stenosis. J Thorac Cardiovasc Surg. 1973;66:404–19.
56. Williams JC, Barratt-Boyes BG, Lowe JB. Supravalvular aortic stenosis. Circulation. 1961;24:1311–8.
57. Brooke BS, Bayes-Genis A, Li DY. New insights into elastin and vascular disease. Trends Cardiovasc Med. 2003;13:176–81.
58. Ewart AK, Jin W, Atkinson D, Morris CA, Keating MT. Supravalvular aortic stenosis associated with a deletion disrupting the elastin gene. J Clin Invest. 1994;93:1071–7.
59. O'Connor WN, Davis JB, Geissler R, Cottrill CM, Noonan JA, Todd EP. Supravalvular aortic stenosis. Clinical and pathologic observations in six patients. Arch Pathol Lab Med. 1985;109: 179–85.
60. Stamm C, Li J, Ho SY, Redington AN, Anderson RH. The aortic root in supravalvular aortic stenosis: the potential surgical relevance of morphologic findings. J Thorac Cardiovasc Surg. 1997; 114:16–24.
61. Jureidini SB, Marino CJ, Singh GK, Fiore A, Balfour IC. Main coronary artery and coronary ostial stenosis in children: detection by transthoracic color flow and pulsed Doppler echocardiography. J Am Soc Echocardiogr. 2000;13:255–63.
62. Firstenberg MS, Greenberg NL, Lin SS, Garcia MJ, Alexander LA, Thomas JD. Transesophageal echocardiography assessment of severe ostial left main coronary stenosis. J Am Soc Echocardiogr. 2000;13:696–8.
63. Sobkowicz B, Hirnle T, Dobrzycki S, Frank M, Sawicki R. Intraoperative echocardiographic assessment of the severe isolated ostial stenosis of left main coronary artery before and after surgical patch angioplasty. Eur J Echocardiogr. 2005;6:280–5.
64. Donofrio MT, Engle MA, O'Loughlin JE, et al. Congenital aortic regurgitation: natural history and management. J Am Coll Cardiol. 1992;20:366–72.
65. Bonow RO, Carabello BA, Chatterjee K, et al. ACC/AHA 2006 guidelines for the management of patients with valvular heart disease: a report of the American College of Cardiology/American Heart Association Task Force on Practice Guidelines (writing Committee to Revise the 1998 guidelines for the management of patients with valvular heart disease) developed in collaboration with the Society of Cardiovascular Anesthesiologists endorsed by the Society for Cardiovascular Angiography and Interventions and the Society of Thoracic Surgeons. J Am Coll Cardiol. 2006;48:e1–148.
66. Enriquez-Sarano M, Tajik AJ. Clinical practice. Aortic regurgitation. N Engl J Med. 2004;351:1539–46.
67. le Polain de Waroux J-B, Pouleur A-C, Goffinet C, et al. Functional anatomy of aortic regurgitation: accuracy, prediction of surgical repairability, and outcome implications of transesophageal echocardiography. Circulation. 2007;116:I264–9.
68. Tweddell JS, Pelech AN, Frommelt PC, et al. Complex aortic valve repair as a durable and effective alternative to valve replacement in children with aortic valve disease. J Thorac Cardiovasc Surg. 2005;129:551–8.
69. Zoghbi WA, Enriquez-Sarano M, Foster E, et al. Recommendations for evaluation of the severity of native valvular regurgitation with two-dimensional and Doppler echocardiography. J Am Soc Echocardiogr. 2003;16:777–802.
70. Lancellotti P, Tribouilloy C, Hagendorff A, et al. European Association of Echocardiography recommendations for the assessment of valvular regurgitation. Part 1: aortic and pulmonary regurgitation (native valve disease). Eur J Echocardiogr. 2010;11:223–44.
71. Friedrich AD, Shekar PS. Interrogation of the aortic valve. Crit Care Med. 2007;35:S365–71.
72. Tribouilloy CM, Enriquez-Sarano M, Fett SL, Bailey KR, Seward JB, Tajik AJ. Application of the proximal flow convergence method to calculate the effective regurgitant orifice area in aortic regurgitation. J Am Coll Cardiol. 1998;32:1032–9.
73. Honjo O, Kotani Y, Osaki S, et al. Discrepancy between intraoperative transesophageal echocardiography and postoperative transthoracic echocardiography in assessing congenital valve surgery. Ann Thorac Surg. 2006;82:2240–6.
74. Tweddell JS, Pelech AN, Jaquiss RDB, et al. Aortic valve repair. Semin Thorac Cardiovasc Surg Pediatr Card Surg Annu. 2005:112–21.
75. Marino BS, Pasquali SK, Wernovsky G, et al. Accuracy of intraoperative transesophageal echocardiography in the prediction of future neo-aortic valve function after the Ross procedure in children and young adults. Congenit Heart Dis. 2008;3:39–46.

76. Dietz HC, Pyeritz RE, Hall BD, et al. The Marfan syndrome locus: confirmation of assignment to chromosome 15 and identification of tightly linked markers at 15q15-q21.3. Genomics. 1991;9:355–61.
77. Boileau C, Jondeau G, Mizuguchi T, Matsumoto N. Molecular genetics of Marfan syndrome. Curr Opin Cardiol. 2005;20: 194–200.
78. Yetman AT, Graham T. The dilated aorta in patients with congenital cardiac defects. J Am Coll Cardiol. 2009;53:461–7.
79. Abe T, Komatsu S. Surgical repair and long-term results in ruptured sinus of Valsalva aneurysm. Ann Thorac Surg. 1988; 46:520–5.
80. Davies RR, Goldstein LJ, Coady MA, et al. Yearly rupture or dissection rates for thoracic aortic aneurysms: simple prediction based on size. Ann Thorac Surg. 2002;73:17–27; discussion 27–8.
81. Thenabadu PN, Steiner RE, Cleland WP, Goodwin JF. Observations on the treatment of dissection of the aorta. Postgrad Med J. 1976;52:671–7.
82. Martinez RM, Anderson RH. Echocardiographic features of the morphologically right ventriculo-arterial junction. Cardiol Young. 2005;15 Suppl 1:17–26.
83. Stamm C, Anderson RH, Ho SY. Clinical anatomy of the normal pulmonary root compared with that in isolated pulmonary valvular stenosis. J Am Coll Cardiol. 1998;31:1420–5.
84. Roberts WC, Shemin RJ, Kent KM. Frequency and direction of interatrial shunting in valvular pulmonic stenosis with intact ventricular septum and without left ventricular inflow or outflow obstruction. An analysis of 127 patients treated by valvulotomy. Am Heart J. 1980;99:142–8.
85. Freedom RM, Yoo SJ. The divided right ventricle. In: Freedom RM, Yoo SJ, Mikailian H, Williams WG, editors. The natural and modified history of congenital heart disease. New York: Blackwell Publishing; 2004. p. 232–5.
86. Restivo A, Cameron AH, Anderson RH, Allwork SP. Divided right ventricle: a review of its anatomical varieties. Pediatr Cardiol. 1984;5:197–204.
87. Pongiglione G, Freedom RM, Cook D, Rowe RD. Mechanism of acquired right ventricular outflow tract obstruction in patients with ventricular septal defect: an angiocardiographic study. Am J Cardiol. 1982;50:776–80.
88. Wong PC, Sanders SP, Jonas RA, et al. Pulmonary valve-moderator band distance and association with development of double-chambered right ventricle. Am J Cardiol. 1991;68:1681–6.
89. Lucas RV, Varco RL, Lillehei CW, Adams P, Anderson RC, Edwards JE. Anomalous muscle bundle of the right ventricle. Hemodynamic consequences and surgical considerations. Circulation. 1962;25:443–55.
90. Hachiro Y, Takagi N, Koyanagi T, Morikawa M, Abe T. Repair of double-chambered right ventricle: surgical results and long-term follow-up. Ann Thorac Surg. 2001;72:1520–2.
91. Simpson WFJ, Sade RM, Crawford FA, Taylor AB, Fyfe DA. Double-chambered right ventricle. Ann Thorac Surg. 1987; 44:7–10.
92. McElhinney DB, Chatterjee KM, Reddy VM. Double-chambered right ventricle presenting in adulthood. Ann Thorac Surg. 2000;70:124–7.
93. Yoshida K, Yoshikawa J, Shakudo M, et al. Color Doppler evaluation of valvular regurgitation in normal subjects. Circulation. 1988;78:840–7.
94. Keane JF, Fyler DC. Pulmonary stenosis. In: Keane JF, Fyler DC, Lock J, editors. Nadas' pediatric cardiology. 2nd ed. Philadelphia: Saunders; 2006. p. 549–58.
95. Veldtman GR, Dearani JA, Warnes CA. Low pressure giant pulmonary artery aneurysms in the adult: natural history and management strategies. Heart. 2003;89:1067–70.
96. Sayger P, Lewis M, Arcilla R, Ilbawi M. Isolated congenital absence of a single pulmonary valve cusp. Pediatr Cardiol. 2000;21:487–9.
97. Mercer-Rosa L, Yang W, Kutty S, Rychik J, Fogel M, Goldmuntz E. Quantifying pulmonary regurgitation and right ventricular function in surgically repaired tetralogy of Fallot: a comparative analysis of echocardiography and magnetic resonance imaging. Circ Cardiovasc Imaging. 2012;5(5):637–43.
98. Bouzas B, Chang AC, Gatzoulis MA. Pulmonary insufficiency: preparing the patient with ventricular dysfunction for surgery. Cardiol Young. 2005;15 Suppl 1:51–7.
99. Gatzoulis MA, Clark AL, Cullen S, Newman CG, Redington AN. Right ventricular diastolic function 15 to 35 years after repair of tetralogy of Fallot. Restrictive physiology predicts superior exercise performance. Circulation. 1995;91:1775–81.
100. Bouzas B, Kilner PJ, Gatzoulis MA. Pulmonary regurgitation: not a benign lesion. Eur Heart J. 2005;26:433–9.
101. Oosterhof T, van Straten A, Vliegen HW, et al. Preoperative thresholds for pulmonary valve replacement in patients with corrected tetralogy of Fallot using cardiovascular magnetic resonance. Circulation. 2007;116:545–51.
102. Geva T. Repaired tetralogy of Fallot: the roles of cardiovascular magnetic resonance in evaluating pathophysiology and for pulmonary valve replacement decision support. J Cardiovasc Magn Reson. 2011;13:1–24.